*energies*

MDPI

*Review*

# Technological Trends for Electrical Machines and Drives Used in Small Wind Power Plants—A Review

**Daniel Fodorean**

Department of Electrical Machines and Drives, Technical University of Cluj-Napoca, 400114 Cluj-Napoca, Romania; daniel.fodorean@emd.utcluj.ro; Tel.: +40-264401828

**Abstract:** High-power-range wind generators mainly employ classical variants, with the advantages of low cost, high robustness and acceptable energetic performance, while for low-power applications, the available electrical drive solutions are more numerous. This paper investigates the current trend in this field, indicating simple or complex structures, with or without self-excitation and with or without mechanical or magnetic transmission. The discussed variants are compared in terms of complexity, cost, fault-tolerance capability and estimated energetic performances but also the grid connectivity for standard conditions. The review is completed by testing options and conditions, as well as the methods for parameter determination, which have an important effect on the controllability of the entire system.

**Keywords:** review; electrical machines and drives; wind power generation



**Citation:** Fodorean, D. Technological Trends for Electrical Machines and Drives Used in Small Wind Power Plants—A Review. *Energies* **2024**, *17*, 6483. https://doi.org/10.3390/en17246483

Academic Editor: Ryszard Palka

Received: 25 November 2024
Revised: 13 December 2024
Accepted: 14 December 2024
Published: 23 December 2024



## 1. Introduction

The "wind power generation" domain is of huge interest today, as, together with other renewable alternatives, it offers an obvious clean option for electric energy generation. The energy management problem and the need to find alternatives to polluting fuels has forced the majority of countries, including those in Europe, the Americas, Asia and Africa, to establish achievable national goals and policies in which, by the year 2050, the use of coal and other fossil fuels is eliminated in the production chain [1,2]. If the target is ambitious, the means of achieving this goal are carefully evaluated along the road. For example, in the case of European countries, the new directive, released in October 2023, states that by the year 2030, at least 27% of produced and used energy across the whole of Europe should be based on renewable energy sources [3]. Similar policies have been announced for American [4,5], African [6] and Asian [7] countries, as well as for the Australian continent [8]. Scientists are at the forefront of this movement, since technology improvement and adequate energy management relies mainly on them.

Just by searching the key term "wind power generation" in scientific paper databases like MDPI, IEEEXplore and ScienceDirect, covering the last 20 years (2005–2024), an impressive number of manuscripts can be found. For example, as of October 2024, in ScienceDirect, the search of the key term results in 137,041 scientific articles (excluding books, chapters, encyclopedias and reviews). Similarly, when searching in IEEEXplore, the search engine displays 72,802 scientific articles (excluding books, courses and standards), while in the case of MDPI, a newer scientific publisher, 7703 scientific articles are included under the "wind power" key term (another 1578 scientific papers are found under the "wind plant" term). This proves that the wind power generation domain is of critical interest.

It is obvious that with such a large amount of literature, determination of the state of the art and the review of technologies used for wind power applications are necessary. And indeed, one can find many scientific reviews with respect to this endeavor [9–25]. Without pretending to present an exhaustive list of reviews, we would like to firstly identify the common elements found in the literature to emphasize the new perspectives presented by

this manuscript. When it comes to reviews on wind power applications, several approaches have been observed. In [9,10], the emphasis is on turbine classification and components, and flying generators are also discussed. In [11], a review on the control techniques of turbines is provided, while an overview of hybrid power generation systems is given in [12]. A review on using advanced numerical methods for the given application is presented in [13]. The influence of mechanical vibration and its mitigation is presented in [14]. In [15,16], the potential of offshore small-scale wind power is evaluated, while in [16], a similar case is discussed, but on a global scale, for future estimations based on a machine learning approach. Also, a review on wind power prediction methods based on artificial intelligence is given in [18]. In [19], a diagnosis approach is presented for the avoidance of common-mode voltage, which negatively impacts the bearing operations of electric generators. A review of the maximization power techniques used in wind power generation is given in [20]. In [21,22], the most studied electrical machine configurations used for power generation are presented. A similar approach is considered in [23,24], but this time with respect to static converters, while in [25], multilevel converters' suitability is also discussed. Thus, a wide variety of related topics have been investigated and reviewed in terms of wind power applications.

Based on accumulated experience in this field over the last 20 years, the present paper proposes a review on technological trends in electrical machines and drive systems used in small wind power plants, applying what can be seen as a systemic approach, with an emphasis on the configuration of the electrical machines and static converters on single or hybrid microgrids. Since we are discussing a small-power-plant application, the investment aspect is not critical, and we can exploit more exotic and complex configurations. Moreover, the testing conditions, which affect the system's parameters (and its controllability), are investigated in this manuscript.

## 2. Electrical Machines Used for Small-Scale Wind Power Generation

### *2.1. Configurations of Electrical Machines Used for Small-Scale Wind Power Plants*

When thinking about the technology involved in wind power generation, its core element is the energy generator, also known as the electrical machine (EM). For high-power plants the solutions are rather limited to very few configurations, mainly due to costs. At the mega-power level, the most common electricity-generation topologies are the synchronous generator (SG), with three-phase stator winding and a field coil placed on the rotor core and fed in dc [26], and the doubly fed induction generator (DFIG) [27–30]. Instead, for small-power plants up to 5 kW, the permanent magnet synchronous generator (PMSG) is already an established solution. Figure 1 presents a wind turbine installed on top of our building, equipped with a PMSG of 700 W (including five pairs of poles and running in a wind speed range of 3–15 m/s).

**Figure 1.** A wind turbine equipped with 700 W PMSG.

In the literature, many permanent magnet configurations are found. The most common one, the surface-mounted permanent magnet synchronous generator (SM-PMSG), has the advantage of providing the best compromise between cost, complexity and robustness [31–35]. Another configuration, the axial flux permanent magnet synchronous generator (AF-PMSG) [36,37], has a better power density ratio as it contains less non-active material. For these two machines, expensive rare-earth materials are typically used (such as NdFeB). To reduce the volume of expensive material, the so-called spoke interior permanent magnet synchronous generator configuration can be considered, which uses low-cost materials (such as ferrite) and the flux concentration technique for increasing the air gap flux of the machine, and has a higher number of magnetic poles. In other applications, flux-switching configurations are considered [38], which use a reduced volume of expensive magnetic material. Moreover, non-active rotor configurations have been studied, such as the switched reluctance machine (SRM) [39–43] or the synchronous reactance machine (SynRM) [44], which need an external exciter such as a capacitor battery pack in a similar way to the autonomous induction generator (AIG) [45]—a squirrel cage induction machine. These last three variants are the cheapest, but have a decreased power density. One of the most complex structures, the transverse flux generator topology, is of *dc* type, uses a polyphase structure, and has perhaps the best power density ratio; it is sometimes also referred to in literature as a Vernier machine [46,47].

Over the last 20 years, different configurations of electrical machines have been investigated in our research laboratory, both with and without excitation on the rotor core or armature. The non-PM-excited structures were first introduced in [45] and are shown in Figure 2. A synchronous generator (SG) with field winding on the rotor core is shown in Figure 2a, demonstrating a common three-phase armature. This structure uses an external *dc* source to produce the main field within the machine. However, when a squirrel cage rotor for an induction machine (the AIG configuration) or a synchronous reluctance generator (SynRG) is used, a *dc* field source is needed without a connection to an external *dc* source. Here, a capacitor pack is used and when the generator reaches speeds beyond the nominal value, the capacitor is charged due to the remanent-induced voltage stored within the stator armature. If the squirrel cage is replaced by three-phase winding in the AIG variant, as shown in Figure 2b, this produces a doubly fed induction generator (DFIG) for which the rotor three-phase winding is fed from an external three-phase *ac* source; if we connect the rotor winding in short-circuit, it will act like a squirrel cage, meaning that it will be seen as a cage machine and will be excited by a capacitor pack [45]. In terms of the SynRG variant, several rotor configurations are possible: the massive rotor core (Figure 2c), which can be equipped with flux barriers or with a reduced volume of permanent magnets made of ceramic or rare-earth (to extend the generator's operation capability); or axially laminated sheets (Figure 2d)—this variant is quite complex from a construction point of view, but it offers the best power factor and variable speed extension capability (here, the flux barriers can also be replaced by PMs to improve the power density of the generator). The next non-PM-excited machine studied was the switched reluctance generator (SRG) (see Figure 2e). Moreover, a modular SRG was also studied (see Figure 2f) [39]. This machine has the advantage of offering very good fault tolerance capability, since each field source coil is magnetically separated from the other coils of the machine. This variant is complex and has a somewhat reduced power density level. All of these variants with no external *dc* source have a very reduced air gap (0.35 mm for the AIG, SG, and SynRG; 0.1 mm for the SRG to increase its power density). Many more PM-excited generator variants were studied due to their improved power density level, which can be a critical criterion for small wind power applications (see Figure 3). Most PM-excited generators are of the synchronous type and include a rare-earth PM (NdFeB, SmCo) as the main field source, named permanent magnet synchronous generators (PMSGs) [34]. For structures with surface-mounted (Figure 3a) or partially inserted (Figure 3b) magnets, a larger air gap is needed, generally 1 mm (since, due to vibrations and shocks, the rotating rotor could touch the stator armature and the entire machine could be compromised). For topologies involving inserted magnets, like

in Figure 3c, this risk is eliminated. Usually, for PM-excited machines, cogging torque is quite important due to the high energy field source stored at a very reduced volume. To reduce the cogging torque, one could use a two-layer three-phase winding configuration with a reduced coil span. If the obtained cogging torque is still too much, it is possible to obtain a smoother induced electromotive force (*emf*) by using a variable height for the PM (see Figure 3c, where, at the corners, the height of the PM is reduced in comparison with the middle part. In the literature, the possibility of using a shift between the axis of two consecutive magnets has been investigated, but since this also produces a shift between the induced voltages, it is not appropriate for wind power applications with a direct grid connection). Of course, one could also use the classic approach of skewing the stator by one slot span (as is usually carried out for AIG, SG, SynRG, etc.), thus producing a smoother *emf*. The three PM-excited variants mentioned previously use expensive rare-earth magnetic materials. To reduce the cost of the power generation system, one could consider using ceramic magnets such as ferrite. However, since such material has a remanent flux density up to three times smaller than rare-earth materials, a specific configuration that doubles the field of the magnets is necessary: the spoke variant (S-PMSG) (see Figure 3d). Next, a rather complex stator armature structure is presented in Figure 3e, known as the claw-pole variant (CP-PMSG)—the electromagnet used here is the well-known car alternator. Next, the axial flux topology (AF-PMSG), shown in Figure 3f, offers a better power density, since its non-active material volume is reduced and there is the option of two stator sides and one inner rotor. The tubular variant (T-PMSG) is shown in Figure 3g for the sake of comparison; it is usually used for wave power generation [47], but with an appropriate transmission adaptation, it can also be considered for wind power plants. Next, the transverse flux permanent magnet generator (TF-PMG) depicted in Figure 3h has the best power density but suffers from complexity and high costs [48].

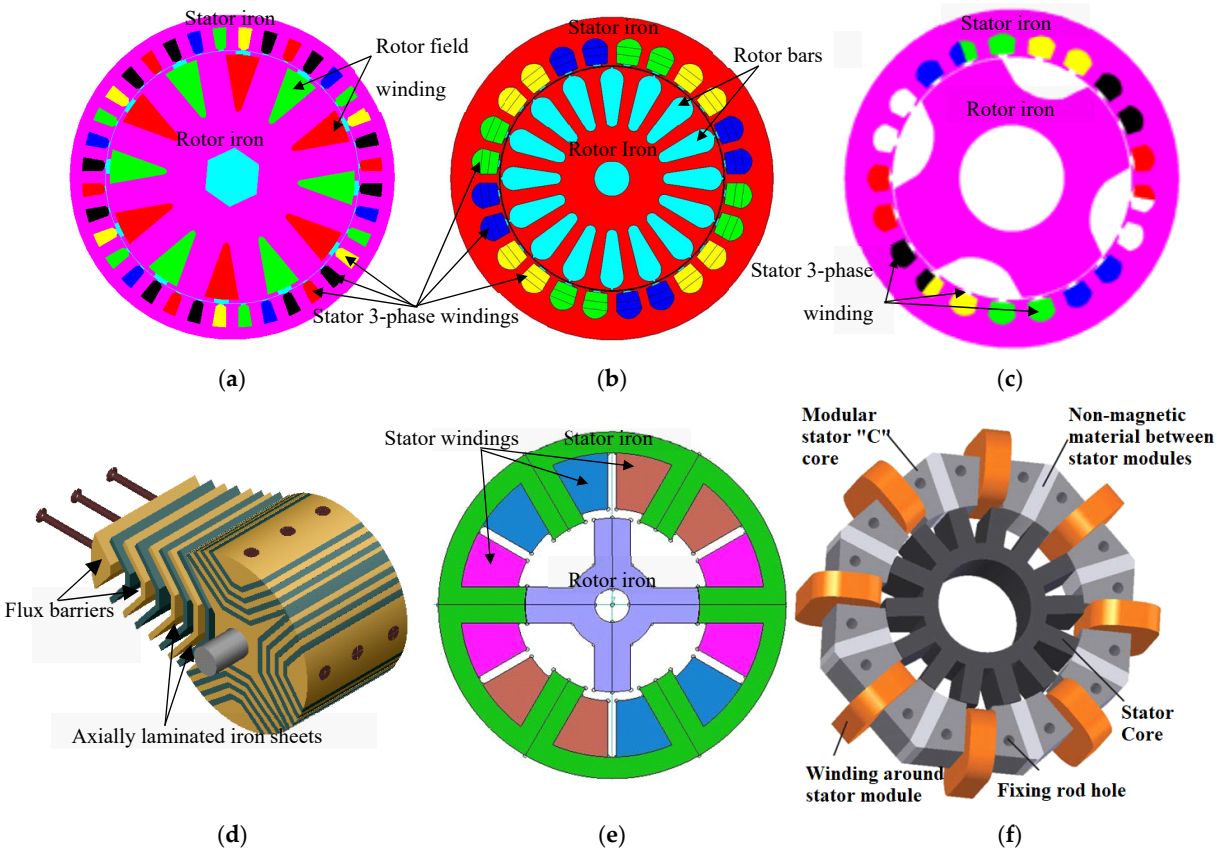


**Figure 2.** Electric generator configurations without permanent magnets: (**a**) SG; (**b**) AIG/DFIG; (**c**) SynRG; (**d**) axially laminated rotor for SynRG; (**e**) standard SRG; (**f**) modular SRG.

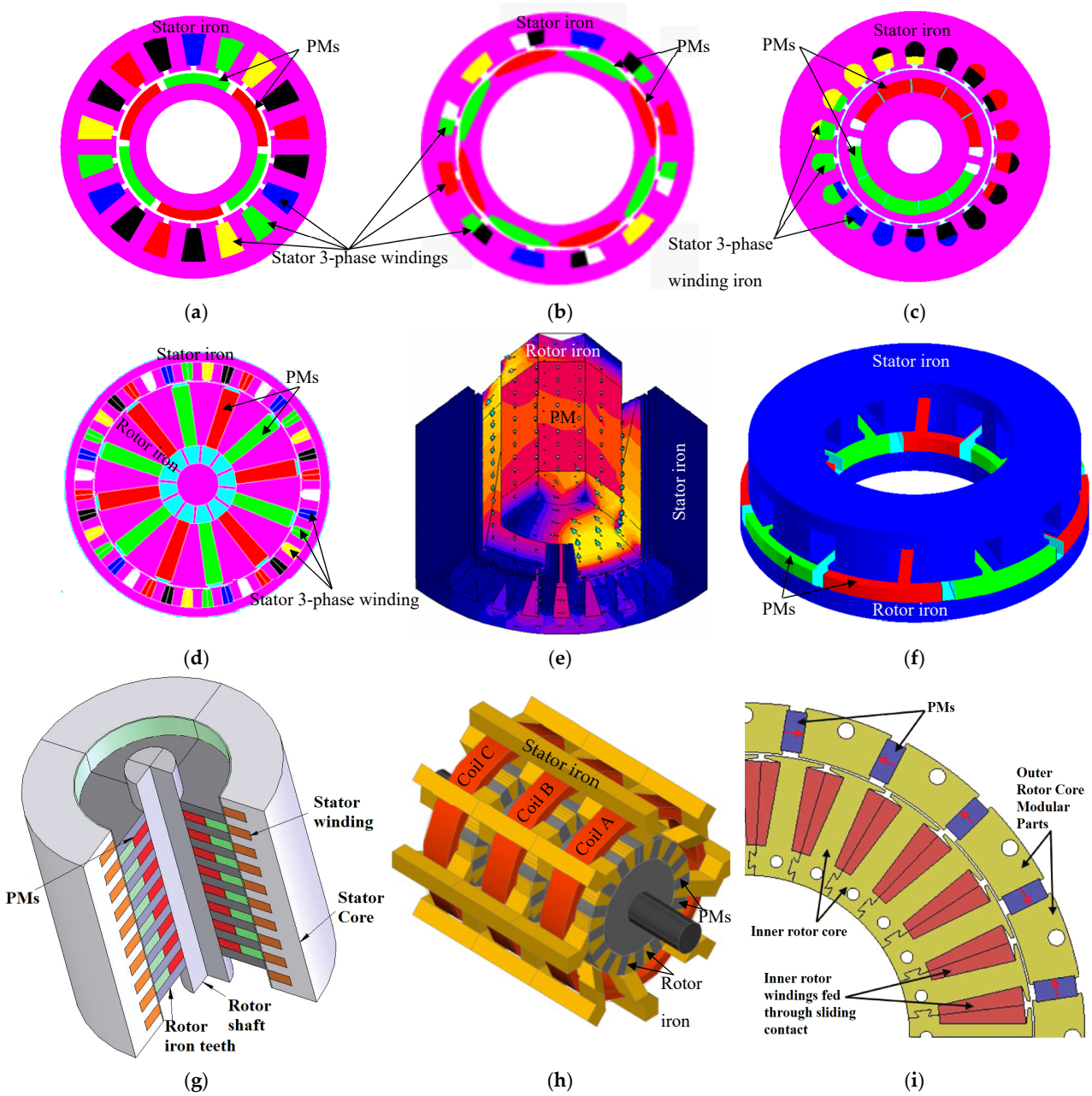


**Figure 3.** Electric generator configurations with permanent magnets: (**a**) PMSG with surface mounted magnets; (**b**) PMSG with half-inserted magnets; (**c**) PMSG with inserted magnets; (**d**) S-PMSG; (**e**) CP-PMSG; (**f**) AF-PMSG; (**g**) T-PMSG; (**h**) TF-PMG; (**i**) CR-PMSG.

Finally, the topology presented in Figure 3i looks like an outer rotor machine (with an inner stator), but this time, both sides of the machine turn in opposite directions [49] and, for this reason, it is called a counter-rotating machine (CR-PMSG). The three-phase winding placed in the inner part of the structure is connected to the load or rectifier via a sliding contact, like the one used to feed the rotor winding of the DFIG [49,50].

With this last variant, we have reached an important complexity level for our generators. Sometimes, a simpler variant could be sufficient for a given application, but for other applications, more complex structures could be more advantageous in small power applications. Thus, next, we explore the possibility of using PMSGs with auxiliary winding, referred to as double excited synchronous generators (DESGs) in the literature [51–53]. Self-excited generators will also be introduced [51,54–56], as well as variants with integrated magnetic gears [57–62].

We have proposed and studied several double excited synchronous machine variants, which have the auxiliary winding placed either on the rotor core or on the stator armature [52,54]. The first variant (Figure 4a) is an "in-wheel" structure (i.e., an outer rotor variant) with PMs mounted on top of the rotor teeth (which also delimit the magnetic poles), which means that the magnets are surface-mounted or placed in the air gap. Moreover, supplementary field winding is placed around the rotor teeth (thus demonstrating a concentrated winding topology), which is then fed from a *dc* external source to control the air gap field. Thus, flux weakening capability is obtained. The stator is a classic *ac* armature with three-phase winding. Another two variants that also have an outer rotor and inner armature stator are depicted in Figure 4b (with surface-mounted magnets) and Figure 4c (with concentrated flux, or the spoke variant). For both variants, supplementary field winding is placed on the stator core, which shares the same slots with the stator winding and is *dc* fed function of the rotor's position. The advantage of these last two options over the first DESG is the lack of sliding contact; however, the geometry, control, and feeding of the field winding are more complex.

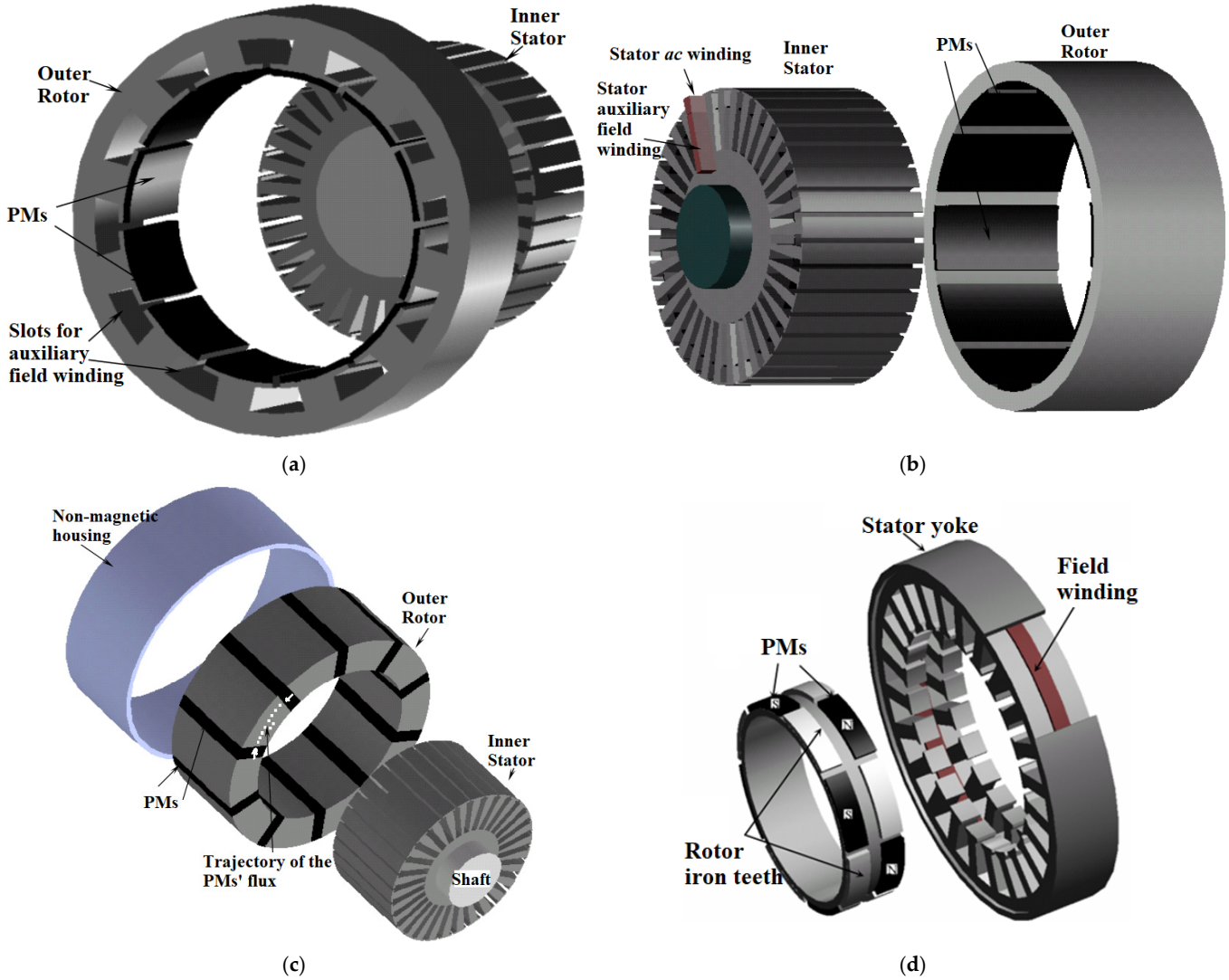


**Figure 4.** DESG studied variants: (**a**) with auxiliary field winding on rotor core (DESG1); (**b**) with auxiliary field winding on stator core, and surface mounted magnets (DESG2); (**c**) with auxiliary field winding on the stator armature and spoke rotor variant (DESG3); (**d**) with homopolar auxiliary winding placed on stator armature (DESG4).

To simplify the feeding of the supplementary winding, a homopolar configuration is employed, as shown in Figure 4d. The winding is *dc*-fed as a function of the necessary flux weakening, and the rotor has consecutive magnetic poles (making it more complex). All four of these DESG variants need a supplementary *dc* source, which involves an increase in both volume and budget for our wind generator power plant. However, the advantage of DESGs is obvious in the case of a lack of wind or excess wind (and if there is no mechanical risk at higher wind speeds). The presence of supplementary winding makes it possible to extend the speed operation capability of the generator [52]. However, to further improve the capability of the DESG for wind power applications, it was necessary to also explore the possibility of using the self-excitation concept.

We designed two synchronous machines with self-excited topologies [54]. The PM is considered to be the main flux source in such cases. The concept of self-excitation means that if the partially induced voltage of the DESG is used to feed the field winding (after being rectified), no extra *dc* power would be needed. It is obvious that by feeding the auxiliary winding, a load should be considered for the stator winding. Hence, the question arises as to how it will affect the generator's operation, or how much electric power is needed to feed the supplementary winding so that it can be used for the load. We know that the power needed to feed the auxiliary winding should produce the rated current for injection into the field winding. Thus, by multiplying the square of the current with the resistance of the field winding, we obtain the amount of power that must be produced by the generator to feed the auxiliary winding. For a 700 W generator, 19 W of electric power is needed to feed the auxiliary winding, which is the equivalent of 2.7% of the generated power; this is quite acceptable, given the fact that we avoided using an external *dc* power source.

The first of the two designed self-excited synchronous generator (SESG) topologies [54], depicted in Figure 5a, has an inner rotor with surface-mounted magnets and field winding around the rotor teeth (like the configuration given in Figure 4a). The second SESG variant, depicted in Figure 5b, has two rotors in axial length, while sharing the same stator armature. The first rotor is the so-called *spoke variant* with ferrite magnets and a flux concentration configuration, similar to the one in Figure 3d, while the second rotor contains an electromagnet (like the one in Figure 2a). Between the rotors is a space necessary for the rotor coil's end-windings.

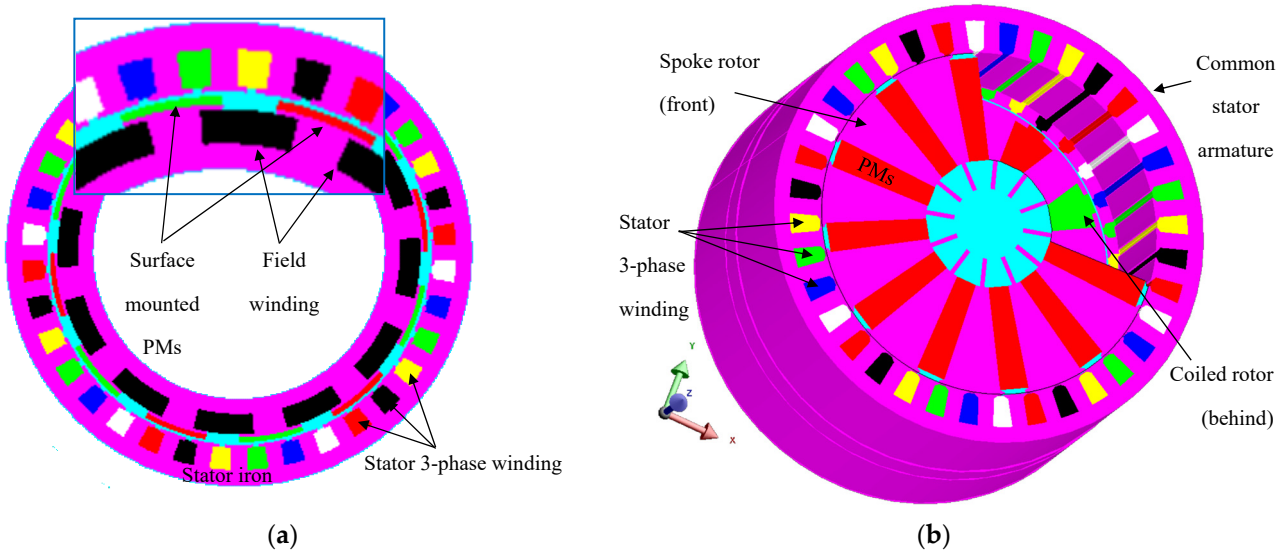


**Figure 5.** SESG studied variants: (**a**) SESG1, with common inner rotor and double excitation on rotor armature; (**b**) SESG2, having two rotors: with spoke magnet part and an electromagnet part, while sharing the same stator armature.

By analyzing these two SESG variants using finite element modeling (FEM), it was observed that SESG1 (Figure 5a) has a very low flux-weakening capability due to its high equivalent air gap (the rare-earth material is more magnetically permeable close to the air), while SESG2 (Figure 5b) has a better flux-weakening capability. This can be seen from the air gap flux density distribution plot in Figure 6: while injecting the rated excitation current into the auxiliary winding for SESG1 (see Figure 6a), due to the high inductance in the direct axis direction, the field-weakening capability is reduced. This is seen at the air gap flux density level, where only 2.45% of the field was modified (this can be increased at a higher current density or under extra cooling, but this involves supplementary losses). Conversely, for SESG2, the electromagnet field is at a level of 78% of the permanent magnet air gap flux (RMS value), resulting in a similar level of flux weakening or flux strengthening. This means that, with the SESG2 variant, the wind speed range can be increased for cases when there is 78% less wind or 78% more wind (but only if there is no mechanical risk to the blades or the entire wind power plant).

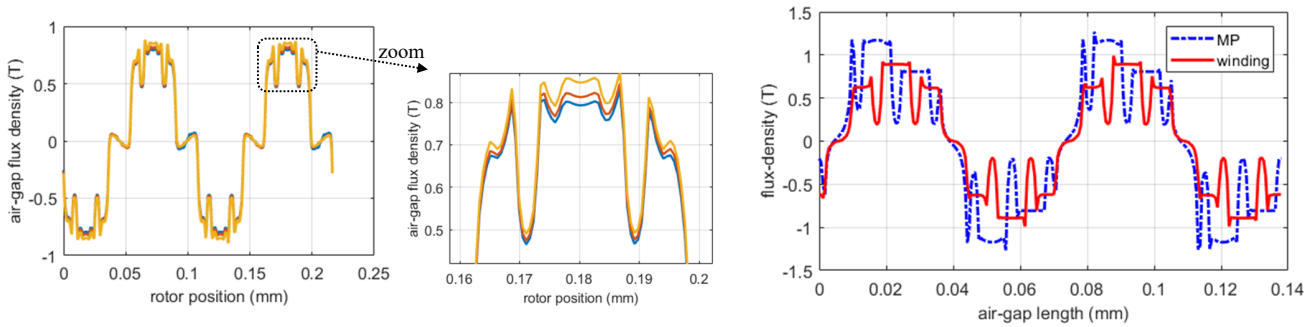


(**a**) (**b**)

**Figure 6.** Flux-density in the airgap while injecting negative current in the auxiliary field winding: (**a**) for SESG1; (**b**) for SESG2.

We have seen that using double-excitation or self-excitation concepts can increase the wind speed operation capability of our generator. This means that we can avoid using a two-stage power electronic system for our wind power plant. Moreover, further improvements can be made to the transmission. Usually, a wind power plant is equipped with a mechanical transmission (see Figure 7a), which involves supplementary volume and cost. However, by integrating the generator with the gear, less volume will be required and the cost of the housing of each power component will be lower. Thus, one solution would be the use of a permanent magnet synchronous generator with an integrated magnetic gear (PMSG-IMG) (see Figure 7b). We studied this concept in Ref. [61].

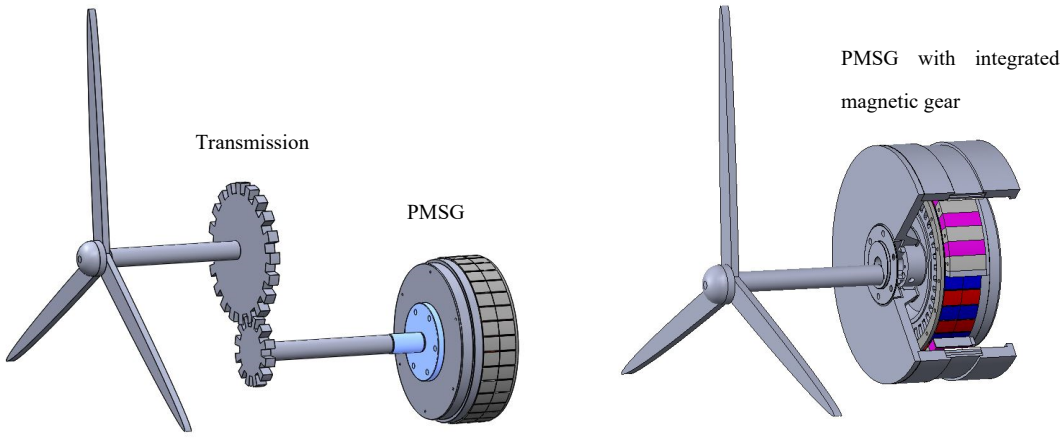


(**a**) (**b**)

**Figure 7.** Wind generator: (**a**) with mechanical transmission; (**b**) with integrated magnetic gear.

It is true that such a solution will increase the cost of the power generator, but the advantage in terms of power density is clearly in its favor. This PMSG-IMG topology was studied, and its cross section is depicted in Figure 8. Here, one can see an ordinary outer rotor PMSG, on top of which is a magnetic gear (a non-magnetic layer is needed in between to avoid any transfer of magnetic flux). The configuration can be specifically designed to obtain the lowest possible torque ripple level (a function of the number of slots and poles for the machine, and a function of the number of poles and static teeth for the magnetic gear). While this is a complex structure, the ability to achieve the best power density (which is critical for small wind power turbines), while integrating the transmission, is a significant advantage that should be considered.

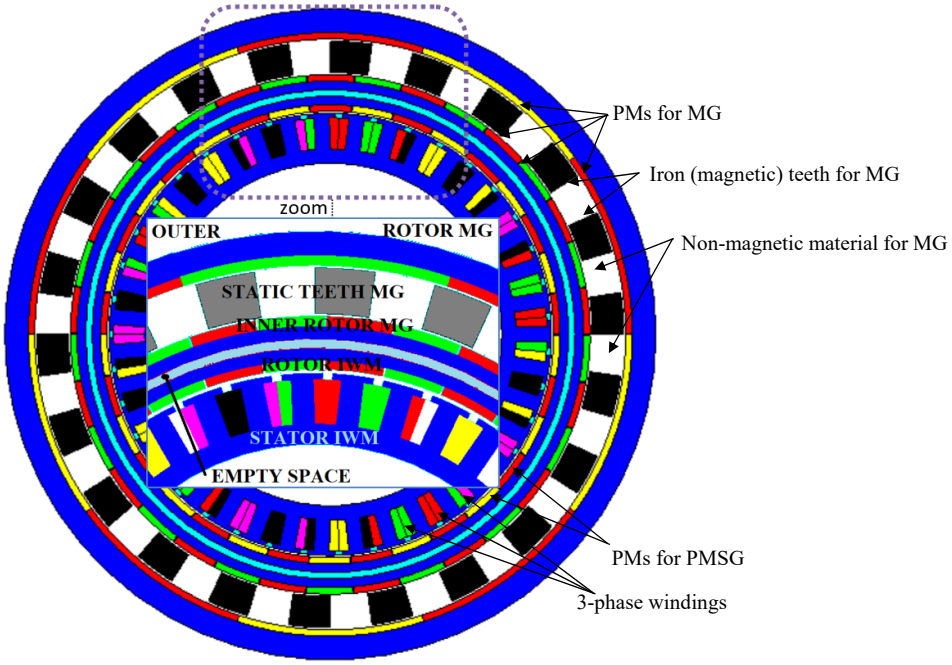


**Figure 8.** Cross-section of the studied PMSG-IMG.

The previously presented structures utilize common three-phase windings; the use of extra-phase variants is now briefly introduced.

### *2.2. Polyphased Systems*

We evaluated several multiphase variants found in the literature [63–70], particularly investigating six-phase and nine-phase PMSG configurations through simulation and tests [71,72]. Polyphase variants are interesting solutions from a fault tolerance point of view; their configuration is obviously more complex and direct grid connectivity is not possible (since the electrical energy produced for all phases needs to be rectified, inverted, filtered, and sent to the microgrid). On the other hand, a six-phase machine can be seen as a double three-phase machine, for which double power can be generated, or, if a fault occurs in the first star winding, the second three-phase winding can be used to maintain the system's operation.

When using polyphase configurations, one can expect to obtain smoother rectified voltage, which means that the filter capacitor, at the output of the rectifier, can be reduced (Figure 9b). Thus, a smoother current and torque can be expected, resulting in less vibration and noise in the generator part (Figure 10b).

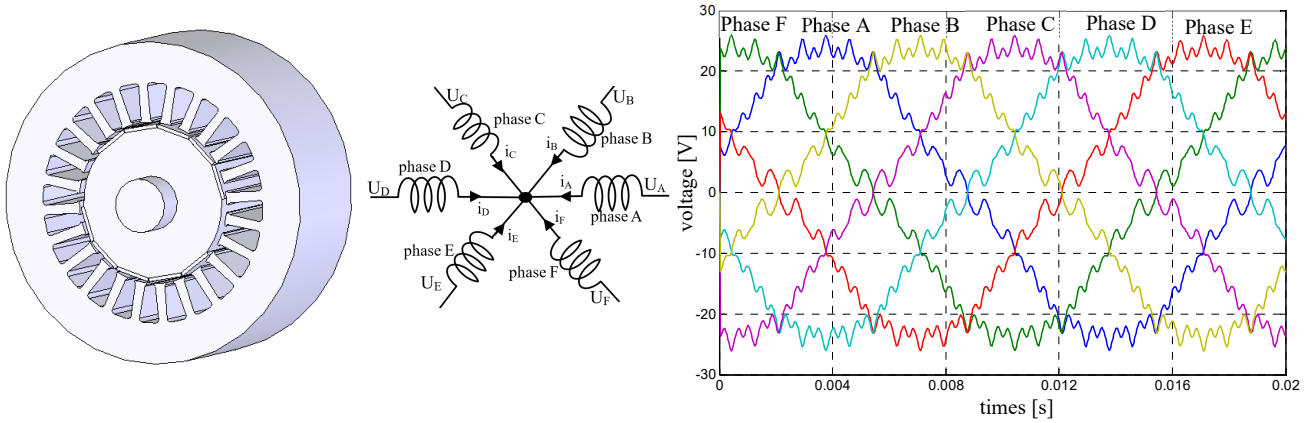


(**a**) (**b**) (**c**)

**Figure 9.** Six-phases PMSG: (**a**) 3D view of the geometry; (**b**) the 6-phase star connection; (**c**) the 6-phases induced *emf*.

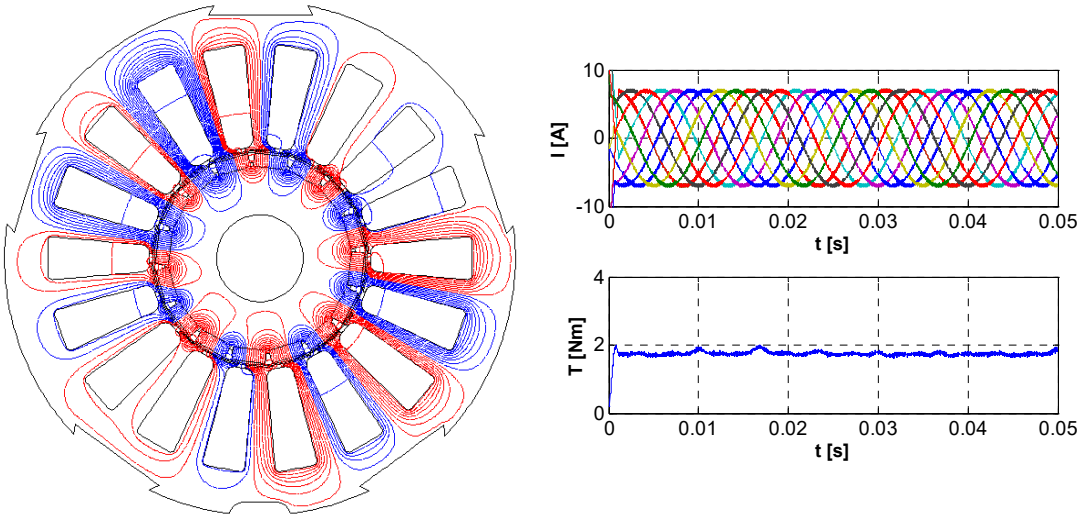


(**a**) (**b**)

**Figure 10.** Nine-phase PMSG: (**a**) field lines (positive & negative poles); (**b**) phase currents (**top**) and torque (**bottom**).

Concerning the electrical machines, no supplementary costs or complexity are expected when dealing with multiphase machines. However, at the power converter level, more complexity and higher costs must be considered. Before evaluating the converter topologies used in wind power applications, we want to emphasize certain elements with respect to the suitability of the discussed electrical machines' configuration for small wind power applications.

### *2.3. Advantages and Disadvantages of Studied Generator Variants*

Here, we present a comparison of the main performances of the discussed electrical generator configurations. The goal of our comparison is not necessarily to decide which electrical generator configuration is the best for wind power plants. Instead, we propose several criteria based on which the generator variants can be compared, while investigating their suitability for the given application. These criteria are depicted in Table 1 and concern the power density of the structures, their capability to operate in a wide speed range (which is translated into wind speed extension operability), fault tolerance capability, complexity, costs and estimated energetic performances (i.e., power factor and efficiency).

**Table 1.** Discussion on the suitability of the electrical generators for small-wind power applications.

| Generator Type | Power Density | Extended Speed Capability | Fault Tolerance Capability | Complexity | Cost | Power Factor | Efficiency |
|---|---|---|---|---|---|---|---|
| SG (Figure 2a) | − | + | − | + | + | − | − − |
| AIG (Figure 2b) | − | − | − | + | + + | − | − − |
| SynRG (Figure 2c) | − | + | − | + + + | + + + | − − | − − |
| axially laminated SynRG (Figure 2d) | − | + + + | − | − − | − | + | − − |
| SRG (Figure 2e) | − − | + | + | + + + | + + | − − − | − − − |
| modular SRG (Figure 2f) | − − − | + | + + + | − − | − − | − − − | − − − |
| surface mounted PMSG (Figure 3a) | + + | − − − | − − − | − | − | − | + + + |
| half-inserted PMSG (Figure 3b) | + | − − | − − − | + | − | − | + + + |
| inserted PMSG (Figure 3c) | + | − | − − − | + | − | + | + + + |
| S-PMSG (Figure 3d) | + | + | − − − | + | + | + | + + |
| CP-PMSG (Figure 3e) | − | + | − − − | − − | − − | − | − − |
| AF-PMSG (Figure 3f) | + + | − − − | − − − | − | − | − | + + |
| T-PMSG (Figure 3g) | − − − | − − − | − − − | − − − | − − | − | − |
| TF-PMG (Figure 3h) | + + + | − − − | − − − | − − | − − | − − | − − |
| CR-PMSG (Figure 3i) | + | + | + | − − | − − | − | − |
| DESG1 (Figure 4a) | + | − | − − | − | − | − | + |
| DESG2 (Figure 4b) | − | + | − − | − − | − − | − | − |
| DESG3 (Figure 4c) | − | + | − − | − − | − − | + | − |
| DESG4 (Figure 4d) | + | + | − − | − − | − − | − − | − − |
| SESG1 (Figure 5a) | + | − | − − | − − − | − | − | + + |
| SESG2 (Figure 5b) | − | + + | − | − − − | + | + | + |
| PMSG-IMG (Figure 8) | + + | + | − − − | − − − | − − − | − | + |
| 6-phases PMSG (Figure 9a) | + | − − − | + + | + | − | − | + + + |
| 9-phases PMSG (Figure 10a) | + | − − − | + + + | + | − | − | + + + |

+ = good; + + = better; + + + = the best/ − = bad; − − = worse; − − − = the worst.

In the next section, the main static converter topologies used in wind power applications will be presented.

## 3. Power Converters and Grid Connectivity in Small Wind Power Applications

The positioning of the power electronic equipment within a wind power plant is depicted in Figure 11.

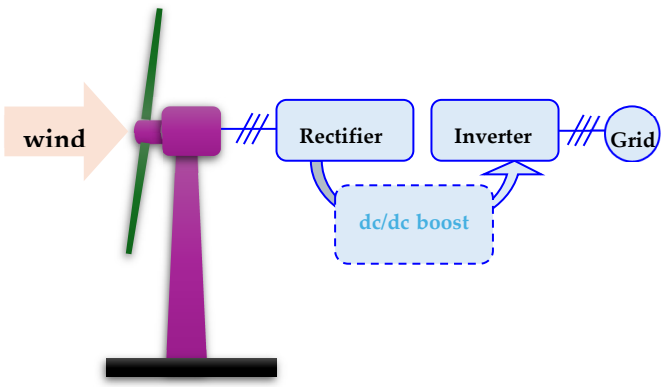


**Figure 11.** The components of the wind power plant, and the necessity of power electronic equipment.

As can be seen from Figure 11, if the electric generator is placed within the turbine, the electronic equipment, especially for small wind power applications, is installed separately. For mono- or three-phase microgrids, at least one rectifier and an inverter are used to ensure the grid connectivity of the electric generator, while a *dc*/*dc* boost converter is not always necessary [23–25,73–77].

### *3.1. Power Converters for Mono-Phase Grid Connection*

The output of a three-phase electric generator (in a star connection for the sake of presentation) is connected to a three-phase rectifier [23] like the one depicted in Figure 12a. After its filter, a boost converter can be used [23,24]: a classic one, like in Figure 12b, or an interleaved configuration [78–81], like the one shown in Figure 12c, to ensure the appropriate input voltage at the monophase inverter. The monophase inverter (an H-bridge configuration like the one in Figure 12d) can be accompanied by a monophase transformer for galvanic isolation [77,79,81]. The *dc*/*dc* boost is not always needed if a generator with a wide speed range capability is used [77], like the SESG or PMSG-IMG variants.

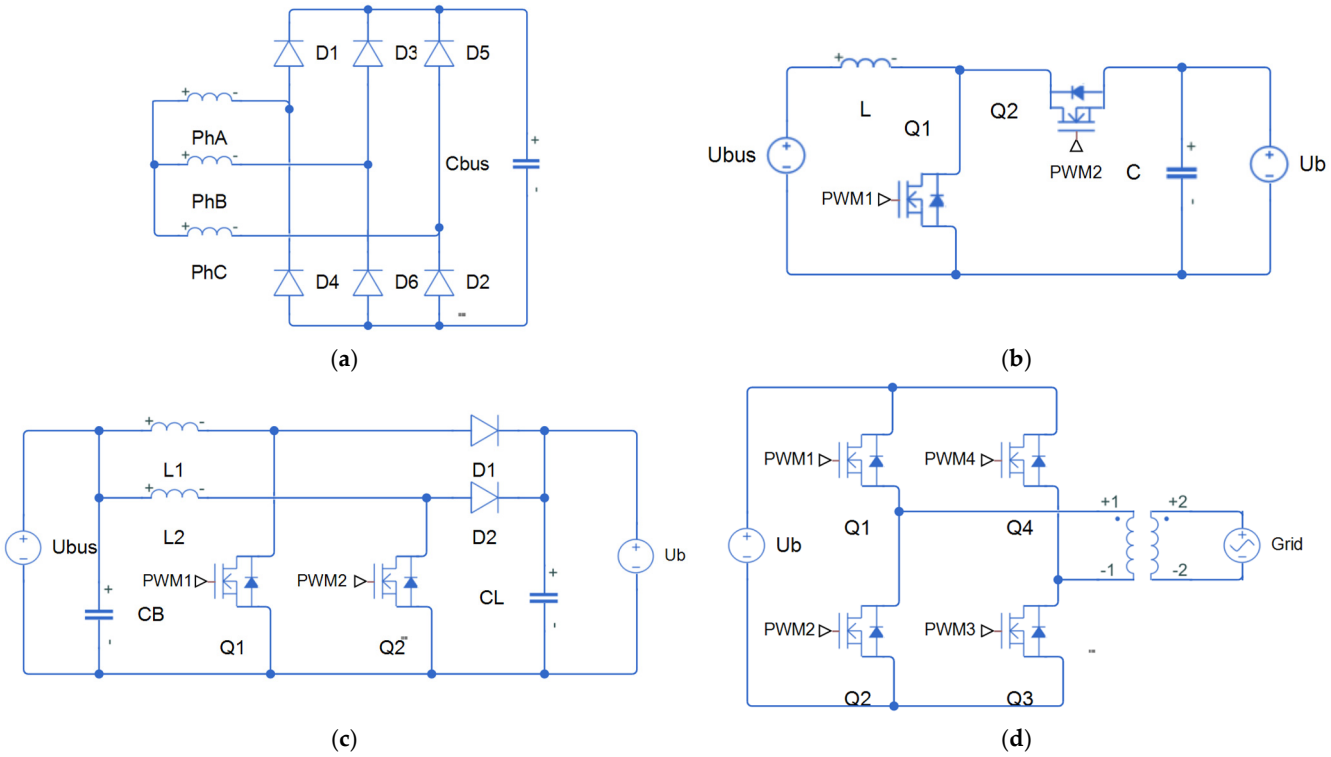


**Figure 12.** Converters used in small wind power plants: (**a**) 3-phase rectifier; (**b**) classic *dc* boost converter; (**c**) interleaved *dc* boost converter; (**d**) H-bridge converter (mono-phased inverter) with transformer (for galvanic insulation).

Even under insulated operating conditions, a three-phase microgrid will usually be put in place to ensure all energy necessities for a domestic facility. Thus, polyphase converters (and inverters) suitable for wind power applications are further presented.

### *3.2. Multilevel Inverters*

In Figure 13, the main multilevel inverter configurations suitable for wind power applications are presented. The common three-phase inverter, with two voltage levels per phase, must be accompanied by an adequate filter, typically of LCL type, that is able to connect the generator to the microgrid [82].

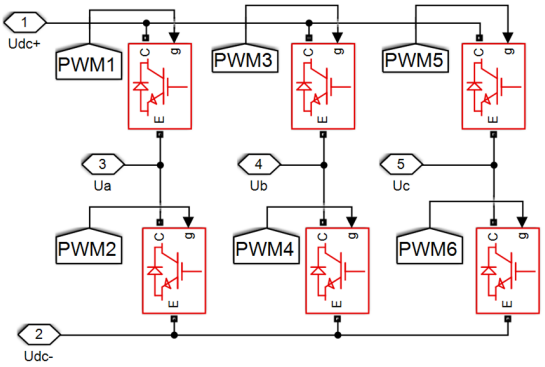


(**a**)

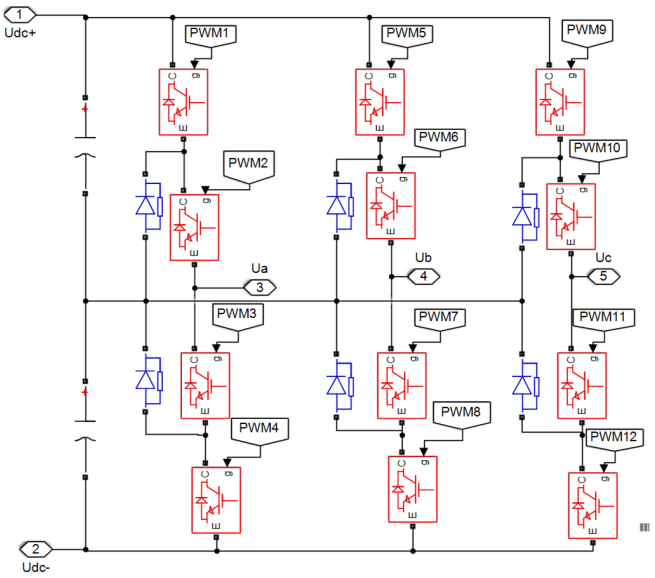


(**b**)

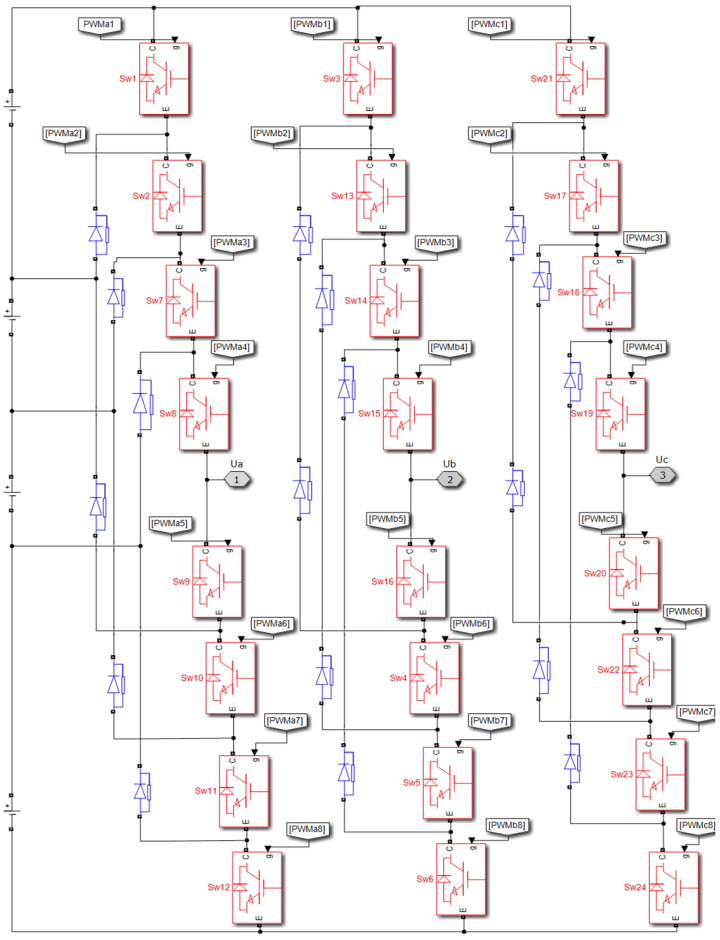


(**c**)

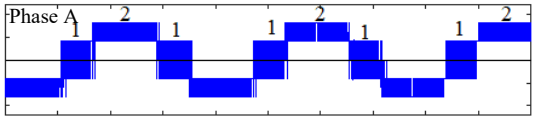


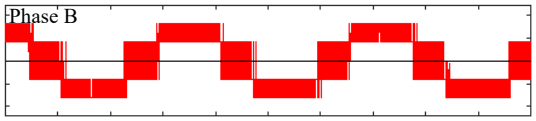


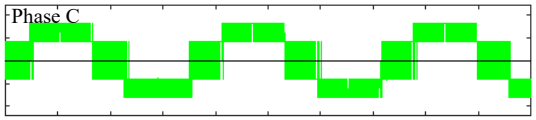


(**d**)

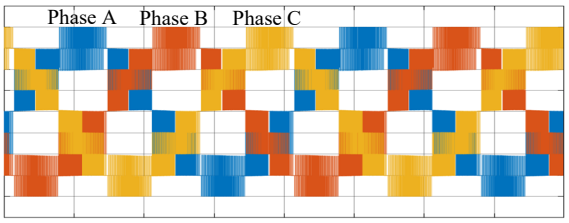


(**e**)

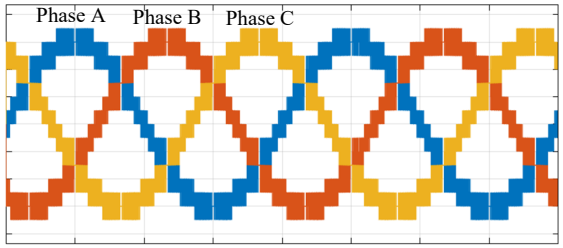


(**f**)

**Figure 13.** Multilevel inverters and their voltage profiles: (**a**) 3-phase two-level inverter; (**b**) 3-phase three-level inverter; (**c**) 3-phase five-level inverter; (**d**) voltage profile for two-level inverter; (**e**) voltage profile for three-level inverter; (**f**) voltage profile for five-level inverter.

To smoothen the induced sinusoidal voltages and currents and to ensure the appropriate total harmonic distortion (THD) level, the user needs to find the best compromise between the complexity of the inverter structure and the volume and cost of the three-phase filter. If a higher-voltage-level inverter is used, i.e., with three levels [83,84], five levels [85–89], or seven or more levels [90,91], a lower-volume and less costly LCL filter is needed. With the classic three-phase, two-level topology in which six power switches are used (see Figure 13a, which produces the voltage profile given in Figure 13d), one can reach up to 12 switches and 6 diodes (see Figure 13b, which produces the voltage profile given in Figure 13e) for the three-level inverter, or 24 switches and 18 diodes (see Figure 13c, which produces the voltage profile given in Figure 13f) for the five-level inverter, and so on. The function of the accepted inverter complexity can decrease the volume, weight and cost of the LCL filter.

The increase in the number of power switches subsequently increases the burden on the controller. Thus, the user needs to find an appropriate compromise in terms of inverter topology and volume and the cost of the filter, as well as the capability of the controller to operate in real time.

### *3.3. Multiphase Converters*

For systems with more than three phases, the addition of one phase is usually translated into the addition of one power branch to the inverter, like in the case of the six-phase machine illustrated in Figure 14a [71]. Similarly, for a nine-phase electric generator, nine double switch branches are needed. If a special request regarding fault tolerance capability is indicated, the user should use other configurations, like the H-bridge configuration (see Figure 14b) or the classic configuration with an extra leg and double power switches (see Figure 14c) [72].

The *H*-bridge variant depicted in Figure 14b demands 36 power switches, differing from the classic nine-phase inverter that demands 18 switches. Nevertheless, its complexity comes with a very good fault tolerance capability, since each phase can be isolated from the others to avoid any electrical cross-coupling between the phases (and the magnetic cross-coupling is significantly reduced in the case of this nine-phase machine, since each coil is located around one stator tooth). To decrease the number of power switches while ensuring adequate fault tolerance, we propose the configuration shown in Figure 14c. Here, for three phases, besides the 6 necessary power switches, a supplementary leg is added, meaning that for the nine-phase machine shown in Figure 10a, 24 switches are needed (less than 36 and slightly more than 18).

The operation of the nine-phase inverter with a supplementary leg for fault compensation (shown in Figure 14c) was experimentally investigated. For the sake of presentation, only three-phase electric characteristics are depicted in Figure 15. During healthy operating conditions, all three currents are correctly shifted and have the same amplitude and quasi-sinusoidal shape (see Figure 15a). If a fault occurs in one phase, the currents within the other two phases will become antagonistic (see Figure 15b), leading to the braking of the electric generator's rotor. Such an undesirable operation can be avoided by insulating the faulted phase and activating the supplementary leg (containing two power switches from which the potential of the other two healthy phases is controlled), thus compensating for the shift in the phases. The currents are no longer antagonistic (see Figure 15c), so no braking is generated; the generator will produce less energy, but its operation will not be stopped. This configuration is, of course, suitable for any type of three-phase machine (and can also be extrapolated for six-phase electric generators).

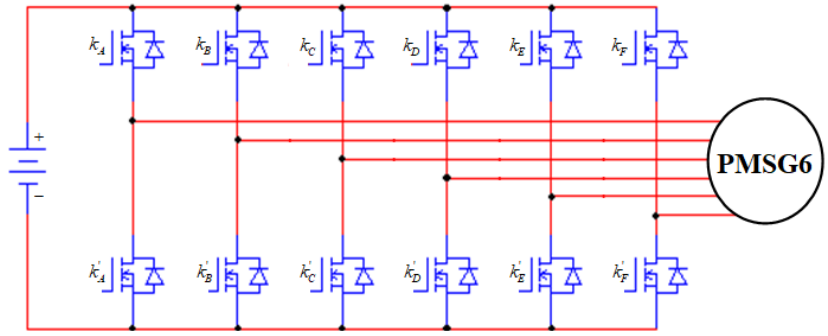


(**a**)

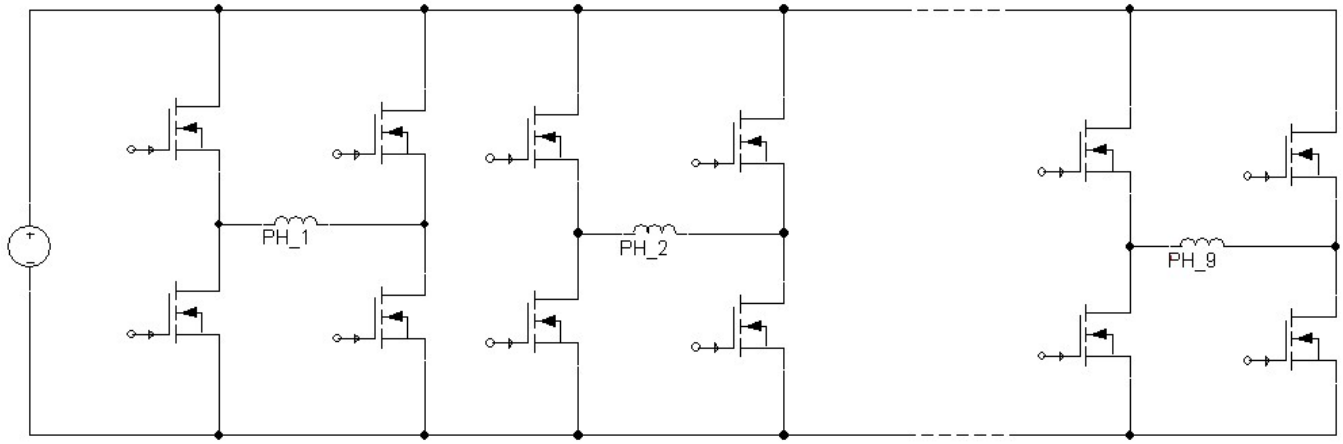


(**b**)

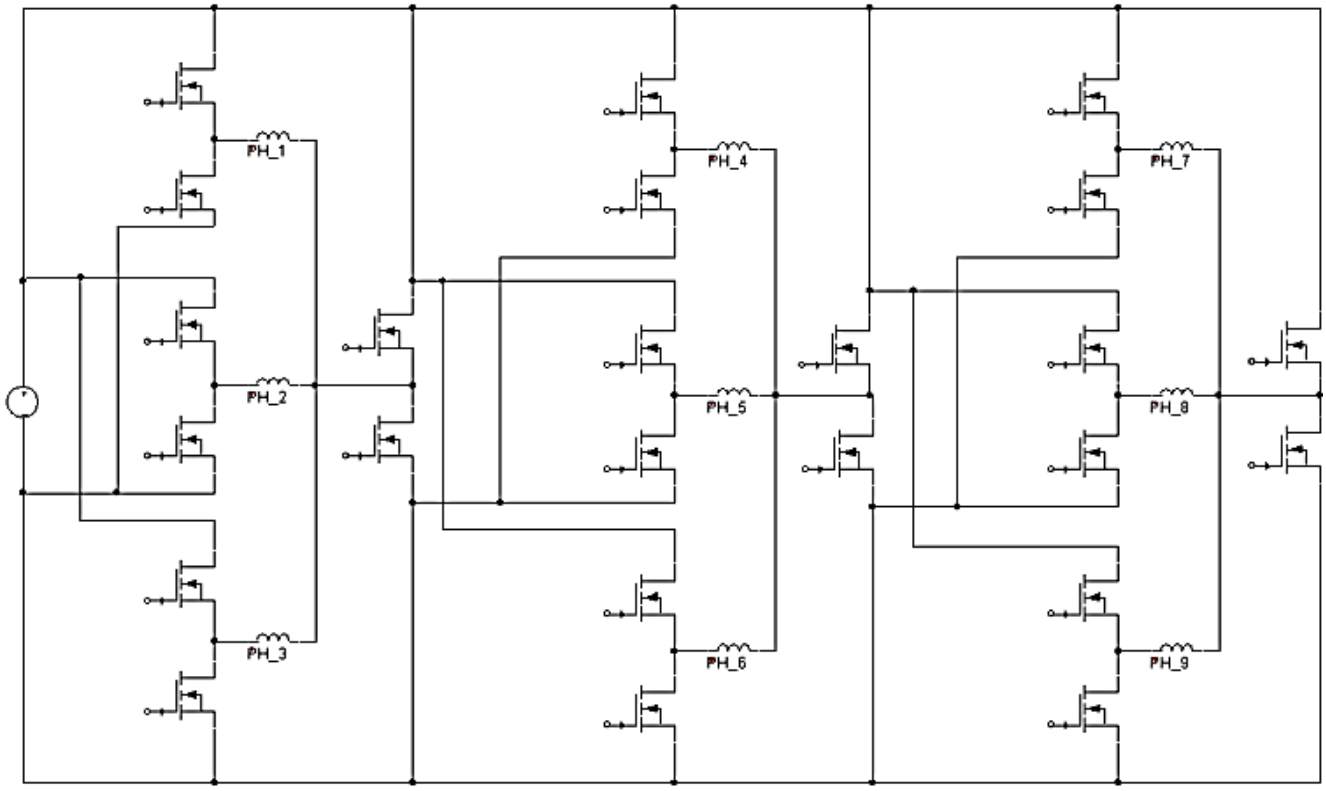


(**c**)

**Figure 14.** Multi-phase power electronic converter structures: (**a**) 6-phase inverter; (**b**) 9-phase *H* bridge inverter; (**c**) 9-phase fault tolerant inverter.

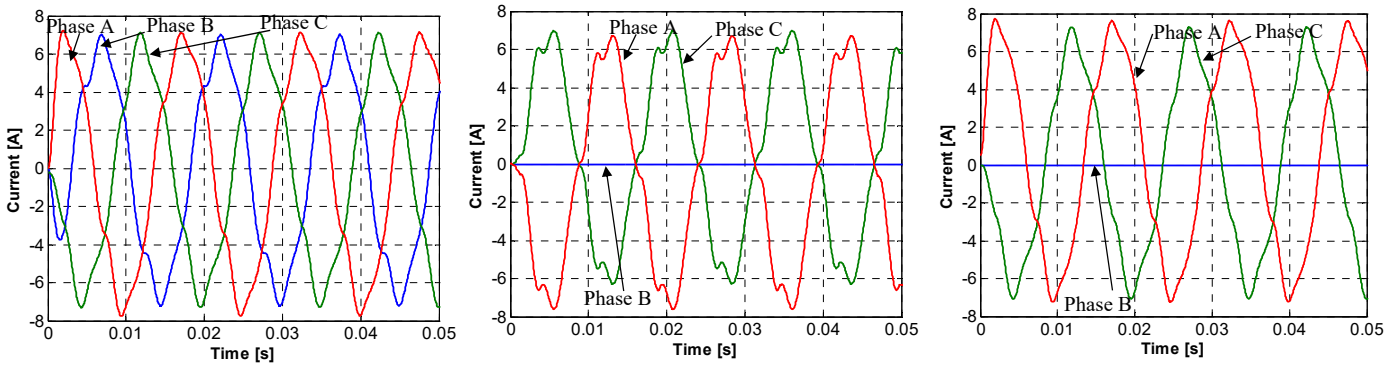


**Figure 15.** The phase currents on one-star of the 9-phase inverter used to feed the 9-phase PMSG: (**a**) healthy case; (**b**) one faulted phase and no compensation; (**c**) faulted phase compensation.

If supplementary voltage is needed for the rectified voltage of our wind power generator, a "Z-source" inverter configuration could be used [91–94]. Here, an impedance (*Z*) is placed between the *dc* source and the three-phase inverter. If the common three-phase inverter produces an output voltage below the input *dc* voltage, the Z-source inverter boosts the input voltage to a desired value. This configuration is depicted in Figure 16, where the *dc* bus at the inverter's input is equipped with two more capacitors and inductances in a "Z" shape (which can also be accompanied by resistances for sensitive filtering improvement). Nevertheless, an LCL filter is still needed at the inverter's output. The number of switches is not increased in this case, which means that there is no supplementary burden on the controller. However, the existence of power capacitors and coils increases the volume, weight and cost of the power converter.

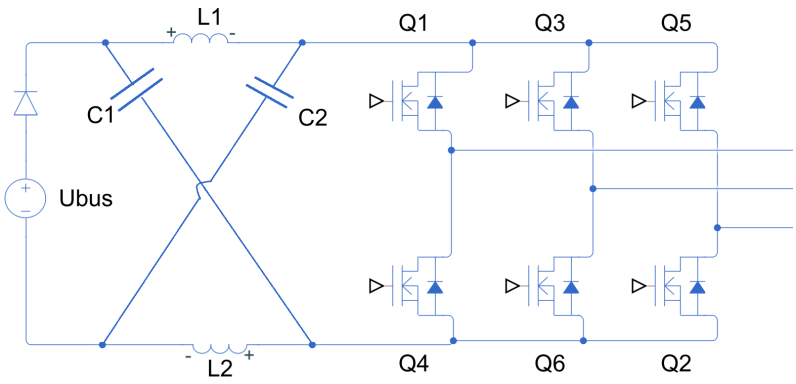


**Figure 16.** Example of Z source three-phase inverter used in wind power generation.

When our wind power plant is used in hybrid power generation systems [95–97], the so-called multisource inverter configurations can be used [98–102]. In fact, the wind generator, with its rectified voltage, offers the primary *dc* source, while a different system provides the secondary source, such as a photovoltaic system [103–106], battery storage unit [105–108], hydrogenator [109,110], biomass system [110], or fuel cell [107,111]. For example, in Figure 17a, the inverter's configuration consists of a two-level inverter with three supplementary switches for each phase. Another variant, with a double three-phase inverter, is illustrated in Figure 17b. Better filtering is expected from the second variant (depicted in Figure 17b). However, having 12 switches with PWM influences the ability of the controller to operate at high frequencies.

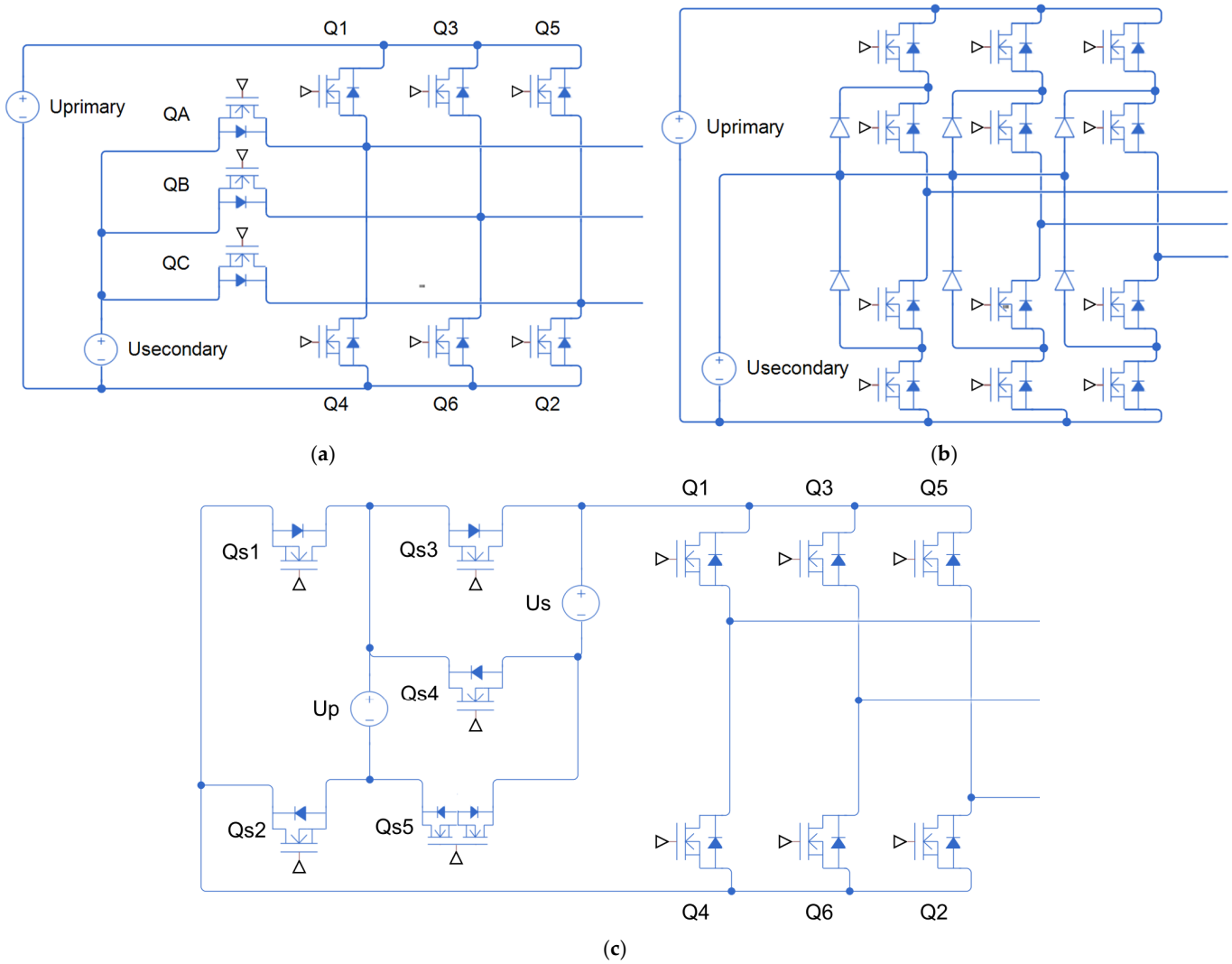


**Figure 17.** Multisource inverter examples: (**a**) with 9 switches; (**b**) with 12 switches & 6 diodes; (**c**) with 11 switches.

Another solution for a multisource inverter with improved efficiency against the previously mentioned variant is depicted in Figure 17c, where no diodes and only 11 switches need to be utilized.

In concluding this discussion on power converters, it should be said that the owner of the wind power plant should decide on the complexity of the system, that is, whether it should involve more than three phases, or whether supplementary power switches and other components are needed to ensure fault tolerance capability. If there are constraints on the volume and weight of the filter, then a multilevel converter is needed. Based on our study, a three-phase, three-level inverter permits the use of a three-phase filter at half of its inductance value, which, as a function of the application, can be an important achievement: the volume, weight and cost of the filter is the highest with respect to the components added to the electrical generator. Thus, a three-phase, three-level inverter could be a good candidate for our wind generator. The use of 12 power switches (and six diodes), like in the case of a three-phase, three-level inverter, does not add too much of a burden on the controller used to generate the PWM signals. This is worth mentioning, since the controller needs to deal with the maximum power point tracking of the wind plant along with the control of the generated electrical energy with the appropriate power factor control, while recovering signals from the voltage and current sensors. This brings

us to the next topic of discussion when dealing with wind power applications: the testing of our power electrical drive.

Table 2 presents several criteria for the base comparison for the introduced static converters and their use in small wind power applications: complexity, cost, higher output voltage capability, fault tolerance capability, estimated efficiency and controllability (or burden on the control unit—microcontroller, DSP, or FPGA). Since only two *dc*/*dc* monophase converters have been introduced (to which a rectifier and a galvanic insulated inverter could be added), in Table 2, only the polyphase converter structures are depicted, and we will leave the reader to decide which topology is best suited for the desired application.

**Table 2.** Discussion on the suitability of the static converters used for small-wind power applications.

| Static Converter Type | Complexity | Cost | Higher Output Voltage | Fault-Tolerance | Efficiency | Controllability |
|---|---|---|---|---|---|---|
| 3-phase 2-level inverter (Figure 13a) | + + + | + + + | − − | − − − | + + + | + + + |
| 3-phase 3-level inverter (Figure 13b) | − − | − − | − | − − | − − | − |
| 3-phase 5-level inverter (Figure 13a) | − − − | − − − | − | − | − − − | − − − |
| 6-phase 2-level inverter (Figure 14a) | − | − − | − | + + | − − | − |
| 9-phase 2-level inverter1 (Figure 14b) | − − − | − − − | − | + + + | − − − | − − − |
| 9-phase 2-level inverter2 (Figure 14c) | − − | − − − | − | + + | − − − | − − |
| Z-source 3-phase inverter (Figure 16) | + + | + + | + | − − − | + + | + + + |
| multi-source inverter1 (Figure 17a) | + | + | + | − | + | + + |
| multi-source inverter2 (Figure 17b) | − − | − | + | − | − − | − |
| multi-source inverter3 (Figure 17c) | − | − | + | − | − | + |

+ = good; + + = better; + + + = the best/− = bad; − − = worse; − − − = the worst.

## 4. Testing of Small Wind Power Generators

### *4.1. Laboratory Setup for Wind Power Generation Testing*

This section depicts the testing conditions of the electrical drive systems used for wind power generation [45,48,112–124]. The power transferred through the blades is emulated by an electric motor (usually a *dc* one). The microgrid is emulated by a variable load (a variable resistor, coil, or capacitor to emulate resistive, inductive, or capacitive loads; a programmable three-phase load can also be considered to emulate the load). Then, depending on the generator's type, extra components can be added if necessary. For example, the electrical scheme used for testing or characterizing autonomous generators is shown in Figure 18a; here, a capacitor pack is needed to auto-excite the electric generator, like the AIG. Figure 18b depicts the synchronous generator testing, either for PMSG characterization (when the dotted line and the *dc* chopper are not needed, since the excitation is through PMs) or SG testing (this time, the chopper and an extra *dc* source are needed to feed the rotor coil). Furthermore, for the case of self-excitation, based on the electrical circuit shown in Figure 18c, the partially generated voltage produced by the wind speed and the primary field source (the PMs) is rectified and reinjected to feed the supplementary winding, which increases the speed range capability of the generator (in our experience, the power needed to feed the auxiliary winding is in the range of 2.7%, which means that this amount of power will not be used for the load, which is negligible and shows the advantage of this topology).

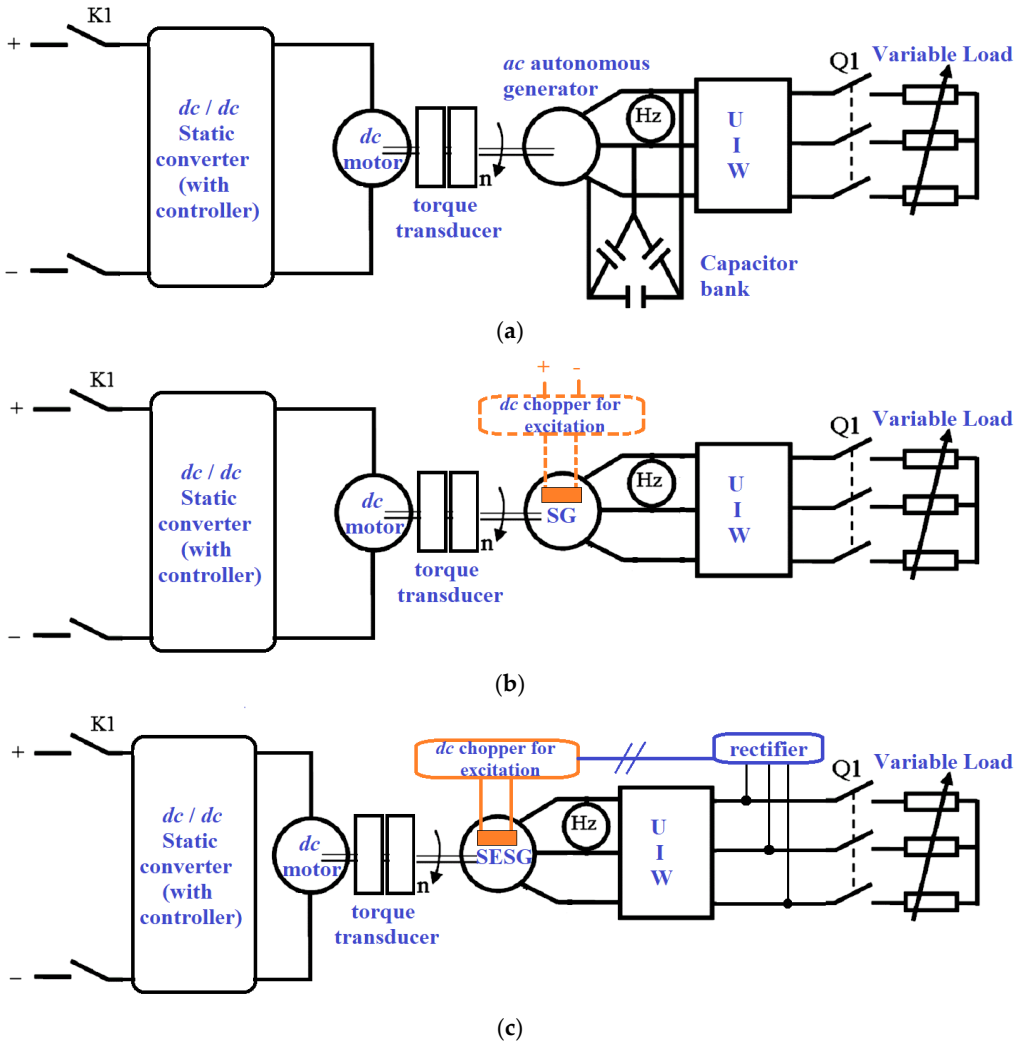


**Figure 18.** Laboratory electric schemes for generator testing: (**a**) autonomous *ac* generators; (**b**) synchronous generators (PMSG and SG with excitation coil); (**c**) self-excited electric generators.

As a case study for wind power generator emulation, we present a testing facility for a PMSG with an integrated magnetic gear (IMG), which is a very new candidate for the given application [60]. The laboratory setup is shown in Figure 19a. Here, an induction motor (IM) is used to emulate the wind turbine. The IM has a shaft connected to our PMSG-IMG via a torque transducer. The induced electromotive force generates three-phase voltages into the winding of the PMSG. This voltage is rectified, filtered, and sent to a programmable load to emulate the microgrid load conditions. The MicroLabBox and a PC *ControlDesk 5.6* software)). The advantage of this PMSG-IMG is the fact that it decreases the input speed by a ratio of 3.4. This means that, even though our PMSG has a high number of pole pairs (17), the frequency will be decreased. The fact that the iron losses are proportional to the square of the frequency means that the PMSG will have reduced iron losses and, consequently, improved efficiency. From Figure 19a, one can see both speeds of the PMSG-IMG (700 r/min for the IMG (outer part) and 205 r/min for the PMSG (inner part)), as well as the induced no-load voltage. In addition, the current and voltage, as well as the torque, are depicted in Figure 19c and Figure 19d, respectively, for load operation. Thus, we have proven the suitability of this PMSG-IMG topology for use in wind power applications. (For PMSG-IMG testing, an electric circuit like the one shown in Figure 18b was used, except the *dc* motor was replaced by an induction motor; we also have an example without the excitation and chopper part.)

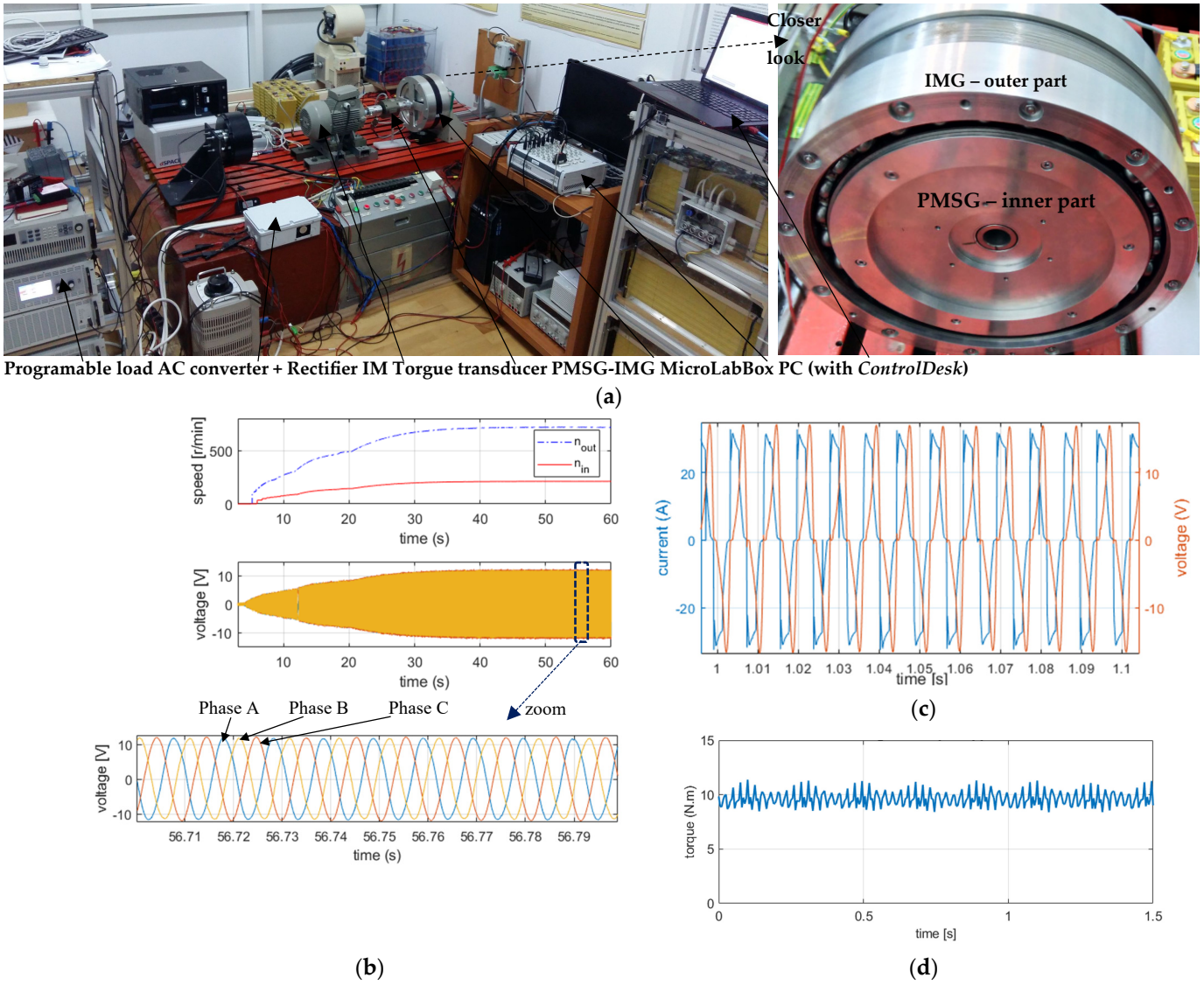


**Figure 19.** Wind power emulator based on PMSG-IMG: (**a**) photography of the laboratory setup (with a closer look on the PMSG-IMG itself); (**b**) speed and voltage characteristics in no-load conditions; (**c**) voltage and current in load conditions; (**d**) torque in load conditions.

### *4.2. Parameters Determination of Electrical Systems Used in Wind Power Generation*

The parameters of the electric generator, converter and filter drastically affect the controllability of the system [125–129]. Researchers are currently evaluating methods to correctly identify the parameters that affect the calculation of coefficients used in current regulators for each type of electrical drive. To employ adequate control, the correct parameters of the electrical drives need to be expressed. Presenting all of the methods and mathematics needed to calculate the parameters of the discussed electrical machines and drives it beyond the scope of this paper (and perhaps more than one manuscript would be needed for this). Here, only a description of the method is given for each discussed parameter, with references or well-established concepts used for parameter determination provided—see Table 3.

**Table 3.** Testing methods for parameters determination in electrical drives used in wind power generators.

| Parameter | Electrical Drive Type | Method |
| --- | --- | --- |
| inductances for induction generator [130–134] | AIG | Short-circuit testing (blocked rotor) |
| $d$ and $q$ axis inductances for synchronous generators [135–141] | SG, PMSG, SESG, PMSG-IMG, SyRG | - Asynchronous starting.<br>- Short-circuit testing (with the output of the stator phases connected to the same potential) in positive orientation (the rotor rotating in the same direction as the rotating field).<br>- Short-circuit testing (with the output of the stator phases connected to the same potential) in negative orientation (the rotor rotating in opposition to the rotating field). |
| $d$ and $q$ axis inductances for synchronous generators [142–147] | SRG | Flux-Current dependency function of the rotor's position. |
| inertia [72,145] | All types of electrical generators | Launching (coasting) method. |
| viscous coefficient [72,145] | All types of electrical generators | Launching (coasting) method. |
| resistance [72,135,143] | All types of electrical generators & inductors used for filtering and boosting | Volt-ampere method. |

## 5. Conclusions

The paper summarizes the current trends in the technology of electrical machines and drives used in small wind power applications. First, classical to more exotic configurations are introduced, from three-phase to more than six-phase topologies with hybrid or self-excitation, mechanical transmission, or magnetic gear integration. Next, based on a review of scientific literature or professional experience and through simulated and experimental results obtained for each of the discussed topologies, the most important performances of the studied electrical generator configurations are introduced. To add more value to the current manuscript, a comparison of these topologies is given in terms of power density, speed capability, fault tolerance, complexity, cost and energetic performance. Similarly, a comparison was made between the reviewed static configuration topologies in terms of complexity, cost, higher output voltage capability, fault tolerance capability, estimated efficiency and controllability (or burden on the control unit—microcontroller, DSP, or FPGA). The goal of this comparison was not to decide on the best option from the author's perspective, but to offer information from which the reader can make a choice based on the application's specificities. A supplementary section was added to indicate the testing conditions for the main types of generator configurations and the methods employed for parameter determination, which affect the controllability of the system.

In terms of future prospects, we expect that the implementation of complex electrical machine topologies and converters will be considered, with fault tolerance capability, for small wind power applications. Even if expensive materials (but with low volume and weight) are used, maximum performance is desirable, especially for insulated microgrids.

Thus, the current review emphasizes the critical aspects that must be considered when choosing an appropriate electrical drive variant suitable for small wind power generation and its characterization and integration in hybrid microgrids.

**Funding:** This research received no external funding.

**Data Availability Statement:** Not applicable.

**Acknowledgments:** The author wants to express his gratitude to all professors who contributed to his professional development, especially to Ioan A. VIOREL, Karoly A. BIRO, Abdesslem DJERDIR and Abdellatif MRAOUI.

**Conflicts of Interest:** The author declares no conflicts of interest.

## References


1. Policies—Global Energy and Climate Model—Analysis—IEA. Available online: https://www.iea.org/reports/global-energy-and-climate-model/policies (accessed on 23 October 2024).
2. 20 RENEWABLE ENERGY Policy Recommendations. Available online: https://iea.blob.core.windows.net/assets/289ce970-b64b-4703-9b1d-e79a422b2ac8/20_Renewable_Energy_Policy_Recommendations.pdf (accessed on 23 October 2024).
3. Directive (EU) 2023/2413 of the European Parliament and of the Council of 18 October 2023 amending Directive (EU) 2018/2001, Regulation (EU) 2018/1999 and Directive 98/70/EC as Regards the Promotion of Energy from Renewable Sources, and Repealing Council Directive (EU) 2015/652. Available online: https://eur-lex.europa.eu/legal-content/EN/TXT/?uri=CELEX:32023L2413&qid=1699364355105 (accessed on 23 October 2024).
4. The Long-Term Strategy of the United States—Pathways to Net-Zero Greenhouse Gas Emissions by 2050. Available online: https://www.whitehouse.gov/wp-content/uploads/2021/10/US-Long-Term-Strategy.pdf (accessed on 23 October 2024).
5. IEA, Latin America Energy Outlook. 2023. Available online: https://iea.blob.core.windows.net/assets/1055131a-8dc4-488b-9e9e-7eb4f72bf7ad/LatinAmericaEnergyOutlook.pdf (accessed on 23 October 2024).
6. Renewable Energy Prospects: June 2020 SOUTH AFRICA. Available online: https://www.irena.org/-/media/Files/IRENA/Agency/Publication/2020/Jun/IRENA_REmap_South_Africa_report_2020.pdf (accessed on 23 October 2024).
7. ASEAN Renewable Energy Policies. August 2016. Available online: https://aseanenergy.org/publications/asean-resp-asean-renewable-energy-policies/ (accessed on 23 October 2024).
8. IEA—Australia 2023 Energy Policy Review. Available online: https://iea.blob.core.windows.net/assets/02a7a120-564b-4057-ac6d-cf21587a30d9/Australia2023EnergyPolicyReview.pdf (accessed on 23 October 2024).
9. Roga, S.; Bardhan, S.; Kumar, Y.; Dubey, S.K. Recent technology and challenges of wind energy generation: A review. *Sustain. Energy Technol. Assess.* **2022**, *52 Pt C*, 102239. [CrossRef]
10. Willis, D.; Niezrecki, C.; Kuchma, D.; Hines, E.; Arwade, S.; Barthelmie, R.; DiPaola, M.; Drane, P.; Hansen, C.; Inalpolat, M. Wind energy research: State-of-the-art and future research directions. *J. Renew. Energy* **2018**, *125*, 133–154. [CrossRef]
11. Baloch, M.H.; Wang, J.; Kaloi, G.S. A review of the state of the art control techniques for wind energy conversion system. *Int. J. Renew. Energy Res.* **2016**, *6*, 1276–1295.
12. Karabacak, K.; Cetin, N. Artificial neural networks for controlling wind–PV power systems: A review. *Renew. Sustain. Energy Rev.* **2014**, *29*, 804–827. [CrossRef]
13. Poompavai, T.; Kowsalya, M. Control and energy management strategies applied for solar photovoltaic and wind energy fed water pumping system: A review. *Renew. Sustain. Energy Rev.* **2019**, *107*, 108–122. [CrossRef]
14. Zuo, H.; Bi, K.; Hao, H. A state-of-the-art review on the vibration mitigation of wind turbines. *Renew. Sustain. Energy Rev.* **2020**, *121*, 109710. [CrossRef]
15. Jaturacherdchaiskul, J.; Thongkeaw, S. Planning and operation for power system with wind power generators: A review. In Proceedings of the 2012 47th International Universities Power Engineering Conference (UPEC), Uxbridge, UK, 4–7 September 2012; pp. 1–5. [CrossRef]
16. Khurshid, H.; Mohammed, B.S.; Al-Yacouby, A.M.; Liew, M.S.; Zawawi, N.A.W.A. Analysis of hybrid offshore renewable energy sources for power generation: A literature review of hybrid solar, wind, and waves energy systems. *Dev. Built Environ.* **2024**, *19*, 100497. [CrossRef]
17. Tuncar, E.A.; Saglam, S.; Oral, B. A review of short-term wind power generation forecasting methods in recent technological trends. *Energy Rep.* **2024**, *12*, 197–209. [CrossRef]
18. Zhu, L. Review of Wind Power Prediction Methods Based on Artificial Intelligence Technology. In Proceedings of the 2024 IEEE 7th Advanced Information Technology, Electronic and Automation Control Conference (IAEAC), Chongqing, China, 15–17 March 2024; pp. 1454–1457. [CrossRef]
19. Liu, Z.; Cheng, X.; Peng, X.; Wang, P.; Zhao, X.; Liu, J.; Jiang, D.; Qu, R. A review of common-mode voltage suppression methods in wind power generation. *Renew. Sustain. Energy Rev.* **2024**, *203*, 114773. [CrossRef]
20. Hannan, M.A.; Al-Shetwi, A.Q.; Mollik, M.S.; Ker, P.J.; Mannan, M.; Mansor, M.; Al-Masri, H.M.K.; Mahlia, T.M.I. Wind Energy Conversions, Controls, and Applications: A Review for Sustainable Technologies and Directions. *Sustainability* **2023**, *15*, 3986. [CrossRef]
21. Aguemon, D.P.; Agbokpanzo, R.G.; Dubas, F.; Vianou, A.; Chamagne, D.; Espanet, C. A Comprehensive Analysis and Review on Electrical Machines in Wind Energy Conversion Systems. *Adv. Eng. Forum* **2020**, *35*, 77–93. [CrossRef]
22. Chen, H.; Zuo, Y.; Chau, K.T.; Zhao, W.; Lee, C.H.T. Modern electric machines and drives for wind power generation: A review of opportunities and challenges. *IET Renew. Power Gener.* **2021**, *15*, 1864–1887. [CrossRef]
23. Souza Junior, M.E.T.; Freitas, L.C.G. Power electronics for modern sustainable power systems: Distributed generation, microgrids and smart grids—A review. *Sustainability* **2022**, *14*, 3597. [CrossRef]
24. Chen, Z.; Guerrero, J.M.; Blaabjerg, F. A Review of the State of the Art of Power Electronics for Wind Turbines. *IEEE Trans. Power Electron.* **2009**, *24*, 1859–1875. [CrossRef]
25. Poorfakhraei, A.; Narimani, M.; Emadi, A. A Review of Multilevel Inverter Topologies in Electric Vehicles: Current Status and Future Trends. *IEEE Open J. Power Electron.* **2021**, *2*, 155–170. [CrossRef]

26. Lipo, T.A.; Du, Z.S. Synchronous motor drives-a forgotten option. In Proceedings of the International Aegean Conference on Electrical Machines & Power Electronics (ACEMP), 2015 Intl Conference on Optimization of Electrical & Electronic Equipment (OPTIM) & 2015 Intl Symposium on Advanced Electromechanical Motion Systems (ELECTROMOTION), Side, Turkey, 2–4 September 2015; pp. 1–5. [CrossRef]
27. Chen, X.; Pan, W.; Wang, X.; Zhou, Y. Design of a Brushless Doubly Fed Generator with Simplified Three-Phase Wound Rotor. *IEEE Trans. Ind. Electron.* **2023**, *70*, 4427–4439. [CrossRef]
28. Shin, K.H.; Lipo, T.A. A super-synchronous doubly fed induction generator option for wind turbine applications. In Proceedings of the IEEE Energy Conversion Congress and Exposition (ECCE), Milwaukee, WI, USA, 18–22 September 2016; pp. 1–7. [CrossRef]
29. Berrueta, A.; Sacristán, J.; López, J.; Rodríguez, J.L.; Ursúa, A.; Sanchis, P. Inclusion of a Supercapacitor Energy Storage System in DFIG and Full-Converter PMSG Wind Turbines for Inertia Emulation. *IEEE Trans. Ind. Appl.* **2023**, *59*, 3754–3763. [CrossRef]
30. Puchalapalli, S.; Singh, B. A novel control scheme for wind turbine driven DFIG interfaced to utility grid. *IEEE Trans. Ind. Appl.* **2020**, *56*, 2925–2937. [CrossRef]
31. Mahmoud, T.; Dong, Z.Y.; Ma, J. Integrated optimal active and reactive power control scheme for grid connected permanent magnet synchronous generator wind turbines. *IET Electr. Power Appl.* **2018**, *12*, 474–485. [CrossRef]
32. Emar, W.; Alzgool, M.; Mansour, I. Reliability Enhancement of a Double-Switch Single-Ended Primary Inductance–Buck Regulator in a Wind-Driven Permanent Magnet Synchronous Generator Using a Double-Band Hysteresis Current Controller. *Energies* **2024**, *17*, 4868. [CrossRef]
33. Putri, R.I.; Pujiantara, M.; Priyadi, A.; Ise, T.; Purnomo, M.H. Maximum power extraction improvement using sensorless controller based on adaptive perturb and observe algorithm for PMSG wind turbine application. *IET Electr. Power Appl.* **2018**, *12*, 455–462. [CrossRef]
34. Fodorean, D.; Derban, S. Design and Performances Evaluation of a PMSG used for Pico-Power Plant—A case study. In Proceedings of the International Conference and Exposition on Electrical and Power Engineering, Iasi, Romania, 20–22 October 2022. [CrossRef]
35. Dranca, M.A.; Chirca, M.; Breban, S.; Fodorean, D. Comparative Design Analysis of Two Modular Permanent Magnet Synchronous Generators. In Proceedings of the 2021 7th International Symposium on Electrical and Electronics Engineering (ISEEE), Galati, Romania, 28–30 October 2021; pp. 1–5. [CrossRef]
36. Gharehseyed, S.; Vahedi, A.; Nobahari, A.; Darjazini, A. Torque characteristics enhancement of ring winding axial flux permanent magnet generator for direct-drive wind turbine. *IET Electr. Power Appl.* **2020**, *14*, 1584–1591. [CrossRef]
37. Pop, A.A.; Jurca, F.; Oprea, C.; Chirca, M.; Breban, S.; Radulescu, M.M. Axial-flux vs. radial-flux permanent-magnet synchronous generators for micro-wind turbine application. In Proceedings of the 2013 15th European Conference on Power Electronics and Applications (EPE), Lille, France, 2–6 September 2013; pp. 1–10. [CrossRef]
38. Seangwong, P.; Fernando, N.; Siritaratiwat, A.; Khunkitti, P. E-Core and C-Core Switched Flux Permanent Magnet Generators for Wind Power Generation. *IEEE Access* **2023**, *11*, 138590–138601. [CrossRef]
39. Szabo, L.; Ruba, M. Segmental Stator Switched Reluctance Machine for Safety-Critical Applications. *IEEE Trans. Ind. Appl.* **2012**, *48*, 2223–2229. [CrossRef]
40. Radimov, N.; Ben-Hail, N.; Rabinovici, R. Switched Reluctance Machines as Three-Phase AC Autonomous Generator. *IEEE Trans. Magn.* **2006**, *42*, 3760–3764. [CrossRef]
41. Sarang, W.A.A.; Memon, A.A. Performance Assessment of Multi-Phase Switched Reluctance Machine for Wind Energy Applications. *Eng. Proc.* **2023**, *46*, 45. [CrossRef]
42. Touati, Z.; Mahmoud, I.; Araújo, R.E.; Khedher, A. Fuzzy Super-Twisting Sliding Mode Controller for Switched Reluctance Wind Power Generator in Low-Voltage DC Microgrid Applications. *Energies* **2024**, *17*, 1416. [CrossRef]
43. Barros, T.A.S.; Neto, P.J.S.; Filho, P.S.N.; Moreira, A.B.; Filho, E.R. An Approach for Switched Reluctance Generator in a Wind Generation System with a Wide Range of Operation Speed. *IEEE Trans. Power Electron.* **2017**, *32*, 8277–8292. [CrossRef]
44. Djouadi, Y.; Tounzi, A.; Idjdarene, K. Effect of Cross-Saturation on the Performance of Synchronous Reluctance Machine Operating as Autonomous Generator. *IEEE Trans. Magn.* **2024**, *60*, 8102705. [CrossRef]
45. Fodorean, D.; Szabo, L.; Miraoui, A. Generator Solutions for Stand Alone Pico-Electric Power Plants. In Proceedings of the International Electrical Machines and Drives Conference (IEMDC 2009), Miami, FL, USA, 3–6 May 2009; pp. 434–438.
46. Ghaheri, A.; Afjei, E.; Torkaman, H. A novel axial air-gap transverse flux switching PM generator: Design, simulation and prototyping. *IET Electr. Power Appl.* **2022**, *17*, 452–463. [CrossRef]
47. Oprea, C.; Martis, C.S.; Jurca, F.; Fodorean, D.; Szabo, L. Permanent Magnet Linear Generator for Renewable Energy Applications: Tubular vs. Four-Sided Structures. In Proceedings of the 3rd International Conference on Clean Electrical Power (ICCEP'11), Ischia, Italy, 14–16 June 2011.
48. Fodorean, D.; Jurca, F.N.; Ruba, M.; Popa, D.C. *Motorization Variants for Light Electric Vehicles—Design, Magnetic, Mechanical and Thermal Aspects*; AlmaMater: Cluj-Napoca, Romania, 2013; ISBN 978-606-504-160-8.
49. Dranca, M.; Chirca, M.; Zaharia, V.; Zaharia, A.; Breban, S. Permanent magnet generator for counter-rotating vertical axis micro-wind turbine. In Proceedings of the International Universities Power Engineering Conference (UPEC), Heraklion, Greece, 28–31 August 2017; pp. 1–6. [CrossRef]
50. Ullah, W.; Khan, F.; Bola Akuru, U. Generating characteristics and experimentation of counter rotating dual rotor wound field flux switching wind generator. *IET Electr. Power Appl.* **2023**, *18*, 153–159. [CrossRef]

51. Rao, Y.T.; Chakraborty, C.; Sengupta, S. Performance and Stability of Brushless Induction Excited Synchronous Generator Operating in Self-Excited Mode for Wind Energy Conversion System. *IEEE Trans. Energy Convers.* **2021**, *36*, 919–929. [CrossRef]
52. Fodorean, D.; Viorel, I.A.; Djerdir, A.; Miraoui, A. Performances for a Synchronous Machine with Optimized Efficiency while Wide Speed Domain is Attempted. *IET Electr. Power Appl.* **2008**, *2*, 64–70. [CrossRef]
53. Amara, Y.; Hlioui, S.; Belfkira, R.; Barakat, G.; Gabsi, M. Comparison of Open Circuit Flux Control Capability of a Series Double Excitation Machine and a Parallel Double Excitation Machine. *IEEE Trans. Veh. Technol.* **2011**, *60*, 4194–4207. [CrossRef]
54. Fodorean, D. Self-Excited Synchronous Machines used for Small Wind Power Applications. In Proceedings of the International Conference on Renewable Energy Research and Applications (ICRERA 2024), Nagasaki, Japan, 9–13 November 2024; pp. 1–6, (ID 131).
55. Zhao, X.; Jiang, J.; Niu, S.; Wang, Q. Slot-PM-Assisted Hybrid Reluctance Generator with Self-Excited DC Source for Stand-Alone Wind Power Generation. *IEEE Trans. Magn.* **2022**, *58*, 8700106. [CrossRef]
56. Izzat, L.F.A.; Heier, S. Development in design of brushless self-excited and self-regulated synchronous generator. In Proceedings of the International Conference on Renewable Energy Research and Applications (ICRERA 2013), Madrid, Spain, 20–23 October 2013; pp. 1024–1029. [CrossRef]
57. Marignetti, F.; D'Aguanno, D.; Di Stefano, R.L. Design and optimization of self-excited synchronous machines with fractional slots. In Proceedings of the International Conference on Ecological Vehicles and Renewable Energies (EVER 2015), Monte Carlo, Monaco, 31 March–2 April 2015; pp. 1–5. [CrossRef]
58. Niu, S.; Liu, Y.; Ho, S.L.; Fu, W.N. Development of a Novel Brushless Power Split Transmission System for Wind Power Generation Application. *IEEE Trans. Magn.* **2014**, *50*, 8203004. [CrossRef]
59. Neves, C.G.C.; Flores, Á.F. Coaxial magnetic gear analysis and optimization. In Proceedings of the International Conference on Renewable Energy Research and Application (ICRERA 2014), Milwaukee, WI, USA, 19–22 October 2014; pp. 91–97. [CrossRef]
60. Jian, L.; Chau, K.T.; Jiang, J.Z. A Magnetic-Geared Outer-Rotor Permanent-Magnet Brushless Machine for Wind Power Generation. *IEEE Trans. Ind. Appl.* **2009**, *45*, 954–962. [CrossRef]
61. Fodorean, D.; Pop Claudia, V. Suitability of a Permanent Magnet Synchronous Generator with Magnetic Gear for Wind Power Generation. In Proceedings of the International Conference on Renewable Energy Research and Applications (ICRERA 2024), Nagasaki, Japan, 9–13 November 2024; pp. 1–6, (ID 242).
62. Yessef, M.; Benbouhenni, H.; Taoussi, M.; Lagrioui, A.; Colak, I.; Bossoufi, B.; Alghamdi, T.A.H. Experimental Validation of Feedback PI Controllers for Multi-Rotor Wind Energy Conversion Systems. *IEEE Access* **2024**, *12*, 7071–7088. [CrossRef]
63. Wang, X.; Ru, Y.; Zhao, H.; Wang, Z. Numerical Investigation of Wind Turbine Airfoil Icing and Its Influencing Factors under Mixed-Phase Conditions. *Energies* **2024**, *17*, 4993. [CrossRef]
64. Kumar, N.; Zakir Husain, M.; Rizwan Khan, M. D, Q reference frames for the simulation of multiphase (six phase) wound rotor induction generator driven by a wind turbine for disperse generation. *IET Electr. Power Appl.* **2019**, *13*, 1823–1834. [CrossRef]
65. Dou, W.; Tong, Y.; Deng, X.; Gao, J.; Yang, F.; Ning, Y.; Zhao, H. Research on Maximum Power Tracking Strategy of 10MW Medium Voltage Six Phase Permanent Magnet Wind Turbine. In Proceedings of the 2020 IEEE International Conference on Applied Superconductivity and Electromagnetic Devices (ASEMD), Tianjin, China, 16–18 October 2020; pp. 1–2. [CrossRef]
66. Han, J.; Zhang, Z. Research on dual-winding permanent magnet generator system with integrated dual-channel controller. *IET Electr. Power Appl.* **2023**, *18*, 42–51. [CrossRef]
67. Meesuk, P.; Kinnares, V. Mathematical Model of Wind Turbine Simulator Based Five Phase Permanent Magnet Synchronous Generator Supplying Non-Linear Loads. In Proceedings of the International Conference on Engineering, Applied Sciences, and Technology (ICEAST), Vientiane, Laos, 1–4 June 2023; pp. 168–171. [CrossRef]
68. Liwei, S.; Bo, Z. Analysis of a new five-phase fault-tolerant doubly salient brushless DC generator. *IET Electr. Power Appl.* **2016**, *10*, 633–640. [CrossRef]
69. Verkroost, L.; Vande Ghinste, A.; Faria da Rocha, L.; De Kooning, J.D.M.; De Belie, F.; Sergeant, P.; Olsen, P.K.; Vansompel, H. Dynamic multi-agent dc-bus reconfiguration in modular motor drives with a stacked polyphase bridge converter. *IET Electr. Power Appl.* **2023**, *18*, 160–173. [CrossRef]
70. Yao, F.; Sun, L.; Sun, D.; Lipo, T.A. Design and Excitation Control of a Dual Three-Phase Zero-Sequence Current Starting Scheme for Integrated Starter/Generator. *IEEE Trans. Ind. Appl.* **2021**, *57*, 3776–3786. [CrossRef]
71. Matyas, A.R.; Biro, K.A.; Fodorean, D. Multi-Phase Synchronous Motor Solution for Steering Applications. *Prog. Electromagn. Res.* **2012**, *131*, 63–80. [CrossRef]
72. Ruba, M.; Fodorean, D. Analysis of Fault-Tolerant Multiphase Power Converter for a Nine-Phase Permanent Magnet Synchronous Machine. *IEEE Trans. Ind. Appl.* **2012**, *48*, 2092–2101. [CrossRef]
73. Katiraei, F.; Iravani, M.R.; Lehn, P.W. Micro-grid autonomous operation during and subsequent to islanding process. *IEEE Trans. Power Deliv.* **2005**, *20*, 248–257. [CrossRef]
74. Al-Shetwi, A.Q.; Hannan, M.; Jern, K.P.; Alkahtani, A.A.; PG Abas, A. Power quality assessment of grid-connected pv system in compliance with the recent integration requirements. *Electronics* **2020**, *9*, 366. [CrossRef]
75. Andresen, B.; Birk, J. A High Power Density Converter System for the Gamesa g10 × 4, 5 mw Wind Turbine. In Proceedings of the 2007 European Conference on Power Electronics and Applications, Aalborg, Denmark, 2–5 September 2007; pp. 1–8.

76. Pigazo, A.; Qin, Z.; Liserre, M.; Blaabjerg, F. Generation of random wind speed profiles for evaluation of stress in WT power converters. In Proceedings of the International Conference on Renewable Energy Research and Applications (ICRERA 2013), Madrid, Spain, 20–23 October 2013; pp. 436–441. [CrossRef]
77. Zhang, Q.; He, J.; Xu, Y.; Hong, Z.; Chen, Y.; Strunz, K. Average-Value Modeling of Direct-Driven PMSG-Based Wind Energy Conversion Systems. *IEEE Trans. Energy Convers.* **2022**, *37*, 264–273. [CrossRef]
78. Li, J.; Xu, H. Direct-Drive Wind Power Generator System Based on Interleaved Boost Converter. In Proceedings of the Asia-Pacific Power and Energy Engineering Conference, Wuhan, China, 27–31 March 2009; pp. 1–4. [CrossRef]
79. Nascimento, A.C.D.; Ribeiro, G.M.S.; de Lima, L.R.; de Alcântara, P.A.; Soares, L.C.S.; Barros, L.S.; Barros, C.M.V. Comparative Analysis between Three-Leg Interleaved and Conventional Bidirectional Converters Applied in Battery of Wind Power-Battery Unit Supplying an Islanded Microgrid. In Proceedings of the IEEE Power & Energy Society General Meeting (PESGM), Seattle, WA, USA, 21–25 July 2024; pp. 1–5. [CrossRef]
80. Mumtaz, F.; Yahaya, N.Z.; Rahman, M.S.; Hasan, M.M. A Non-Isolated High-Gain Non-Inverting Interleaved DC-DC Converter Multi-Output Network for Renewable Energy Application. In Proceedings of the IEEE International Conference on Automatic Control and Intelligent Systems (I2CACIS), Shah Alam, Malaysia, 17 June 2023; pp. 257–262. [CrossRef]
81. Aguirre, M.; Kouro, S.; Rodriguez, J.; Abu-Rub, H. Model predictive control of interleaved boost converters for synchronous generator wind energy conversion systems. In Proceedings of the IEEE International Conference on Industrial Technology (ICIT), Seville, Spain, 17–19 March 2015; pp. 2295–2301. [CrossRef]
82. Szabo, L.; Ruba, M.; Fodorean, D. Study on a Simplified Converter Topology for Fault Tolerant Motor Drives. In Proceedings of the 11th OPTIM'08, Brasov, Romania, 22–24 May 2008; pp. 197–202. [CrossRef]
83. Choudhury, A.; Pillay, P.; Williamson, S.S. Comparative Analysis Between Two-Level and Three-Level DC/AC Electric Vehicle Traction Inverters Using a Novel DC-Link Voltage Balancing Algorithm. *IEEE J. Emerg. Sel. Top. Power Electron.* **2014**, *2*, 529–540. [CrossRef]
84. Fodorean, D.; Ioana, G. Multilevel inverter for EV charging via hybrid storage unit (Fuel Cell, Battery, Ultracapacitor). In Proceedings of the Electrical Systems for Aircraft, Railway, Ship Propulsion and Road Vehicles (ESARS) and International Transportation Electrification Conference (ITEC) 2024, Naples, Italy, 26–29 November 2024; pp. 1–6, *in press*.
85. Farhangi, R.; Barzegarkhoo, R.P.; Aguilera, S.S.; Lee, D.D.; Lu, C.; Siwakoti, Y.P. A Single-Source Single-Stage Switched-Boost Multilevel Inverter: Operation, Topological Extensions, and Experimental Validation. *IEEE Trans. Power Electron.* **2022**, *37*, 11258–11271. [CrossRef]
86. Silva, C.E.; Alzamora, A.M.; Paula, H.D. Broad Comparison of Multilevel Inverter Topologies Operating in Hostile Environments: DC Transmission Applicability and Feasibility. *IEEE Trans. Ind. Appl.* **2022**, *58*, 6852–6863. [CrossRef]
87. Ravi, A.; Manoharan, P.S.; Vijay Anand, J. Modeling and simulation of three phase multilevel inverter for grid connected photovoltaic systems. *Sol. Energy* **2011**, *85*, 2811–2818. [CrossRef]
88. Lizana, R.; Rivera, S.; Figueroa, F.; Flores-Bahamonde, F.; Rodriguez, J.; Goetz, S.M. Hybrid Energy Storage System Based on a Multioutput Multilevel Converter. *IEEE J. Emerg. Sel. Top. Pow. Electron.* **2023**, *11*, 3864–3873. [CrossRef]
89. Jakhar, A.; Sandeep, N.; Verma, A.K. Seven-Level Common-Ground-Type Inverter with Reduced Voltage Stress. *IEEE J. Emerg. Sel. Top. Power Electron.* **2024**, *12*, 2108–2115. [CrossRef]
90. Badawy, M.O.; Sharma, M.; Hernandez, C.; Elrayyah, A.; Guerra, S.; Coe, J. Model Predictive Control for Multi-Port Modular Multilevel Converters in Electric Vehicles Enabling HESDs. *IEEE Trans. Energy Convers.* **2022**, *37*, 10–23. [CrossRef]
91. Thelukuntla, C.S.; Veerachary, M. Resonant controller based single-phase Z-source inverter with LCL-filter. In Proceedings of the Joint International Conference on Power Electronics, Drives and Energy Systems & 2010 Power India, New Delhi, India, 20–23 December 2010; pp. 1–6. [CrossRef]
92. Almeida, F.A.F.; Guerra, F.; Serrão Gonçalves, F.A. Z-Source Inverter for Photovoltaic Microgeneration. In Proceedings of the 2019 IEEE 15th Brazilian Power Electronics Conference and 5th IEEE Southern Power Electronics Conference (COBEP/SPEC), Santos, Brazil, 1–4 December 2019; pp. 1–6. [CrossRef]
93. Wang, X.; Vilathgamuwa, D.M.; Tseng, K.J.; Gajanayake, C.J. Controller design for variable-speed permanent magnet wind turbine generators interfaced with Z-source inverter. In Proceedings of the 2009 International Conference on Power Electronics and Drive Systems (PEDS), Taipei, Taiwan, 2–5 November 2009; pp. 752–757. [CrossRef]
94. Venkatesan, S.G.; Kadwane, S.G.; Samarth, M.P.; Gawande, S.P. Harmonic analysis of grid connected Z-source inverter under variable load/input conditions. In Proceedings of the 2016 IEEE 6th International Conference on Power Systems (ICPS), New Delhi, India, 4–6 March 2016; pp. 1–6. [CrossRef]
95. Saha, P.; Kar, A.; Behera, R.R.; Pandey, A.; Chandrasekhar, P.; Kumar, A. Performance optimization of hybrid renewable energy system for small scale micro-grid. *Mater. Today Proc.* **2022**, *63*, 527–534. [CrossRef]
96. Yao, J.; Guo, L.; Zhou, T.; Xu, D.; Liu, R. Capacity configuration and coordinated operation of a hybrid wind farm with FSIG-based and PMSG-based wind farms during grid faults. *IEEE Trans. Energy Convers.* **2017**, *32*, 1188–1199. [CrossRef]
97. Zhou, L.; Preindl, M. Reconfigurable hybrid micro-grid with standardized power module for high performance energy conversion. *Appl. Energy* **2023**, *351*, 121708. [CrossRef]
98. Zhu, J.; Li, Y.; Peng, F.Z.; Lehman, B.; Huang, H. From Active Resistor to Lossless and Virtual Resistors: A Review, Insights, and Broader Applications to Energy Grids. *IEEE J. Emerg. Sel. Top. Power Electron.* 2024, *early access*. [CrossRef]

99. Hosseinzadeh, M.A.; Sarebanzadeh, M.; Kennel, R.; Babaei, E.; Rivera, M. New Generalized Circuits for Single-Phase Multisource Multilevel Power Inverter Topologies. *IEEE Trans. Power Electron.* **2023**, *38*, 6823–6830. [CrossRef]
100. Singh, D.; Sandeep, N. A Novel Common-Ground Multisource Inverter. *IEEE Trans. Power Electron.* **2023**, *38*, 15142–15146. [CrossRef]
101. Liu, L.; Zhou, D.; Zou, J.; Wang, W. Decoupled Modeling and Wide-Range Power Distribution Strategy for the Multisource Inverter in Microgrids. *IEEE Trans. Power Electron.* **2024**, *38*, 12078–12090. [CrossRef]
102. Zhou, D.; Zhang, Z.; Shen, Z.; Zou, J. Modulated Model Predictive Control of Multisource Inverters with Flexible Power Distribution. *IEEE Trans. Ind. Electron.* **2024**, *71*, 13732–13741. [CrossRef]
103. Kurbatova, T.; Sotnyk, I.; Perederii, T.; Prokopenko, O.; Wit, B.; Pysmenna, U.; Kubatko, O. On-Grid Hybrid Wind–Solar Power Plants in Ukraine's Residential Sector: Economic Justification of Installation Under Different Support Schemes. *Energies* **2024**, *17*, 5214. [CrossRef]
104. Xuewei, S.; Xuefang, S.; Wenqi, D.; Peng, Z.; Hongyan, J.; Jinfang, W.; Yang, W. Research on Energy Storage Configuration Method Based on Wind and Solar Volatility. In Proceedings of the 2020 10th International Conference on Power and Energy Systems (ICPES), Chengdu, China, 25–27 December 2020; pp. 464–468. [CrossRef]
105. Ely, W.; Doumbia, M.L.; Tahar, T.; Betoka, S.P.; Hamza, H. Energy Management of an Autonomous Hybrid Wind-Photovoltaic Microgrid with Battery Storage. In Proceedings of the International Conference on Renewable Energy Research and Applications (ICRERA 2023), Oshawa, ON, Canada, 29 August–1 September 2023; pp. 492–498. [CrossRef]
106. Grgić, I.; Bašić, M.; Vukadinović, D.; Bubalo, M. Optimal Control of a Standalone Wind-Solar-Battery Power System with a Quasi-Z-Source Inverter. In Proceedings of the International Conference on Renewable Energy Research and Application (ICRERA 2020), Glasgow, UK, 27–30 September 2020; pp. 61–66. [CrossRef]
107. Ciochinda, L.C.A.; Fodorean, D. Insulated Hybrid Grid based on PV system, Battery and Fuel Cell car—A case study. *Eng. Proc.* **2024**, *79*, 12. [CrossRef]
108. Sun, X.; He, H.; Ma, L. Harmony search meta-heuristic algorithm based on the optimal sizing of wind-battery hybrid micro-grid power system with different battery technologies. *J. Energy Storage* **2024**, *75*, 109582. [CrossRef]
109. Gade, S.; Agrawal, R.; Munje, R. Recent trends in power quality improvement: Review of the unified power quality conditioner. *ECTI Trans. Electr. Eng. Electron. Commun.* **2021**, *19*, 268–288. [CrossRef]
110. Kablar, N.A. Renewable energy: Wind turbines, solar cells, small hydroelectric plants, biomass, and geothermal sources of energy. *J. Energy Power Eng.* **2019**, *13*, 162–172.
111. Li, D.; Qian, K.; Gao, C.; Xu, Y.; Xing, Q.; Wang, Z. Research on Electric Hydrogen Hybrid Storage Operation Strategy for Wind Power Fluctuation Suppression. *Energies* **2024**, *17*, 5019. [CrossRef]
112. Ma, K.; Yang, Y.; Wang, H.; Blaabjerg, F. Design for Reliability of Power Electronics in Renewable Energy Systems. In *Use, Operation and Maintenance of Renewable Energy Systems*; Springer: Berlin/Heidelberg, Germany, 2014; pp. 295–338.
113. Obando Vega, F.; Rubio-Clemente, A.; Chica, E. Control System for the Performance Analysis of Turbines at Laboratory Scale. *Energies* **2024**, *17*, 4950. [CrossRef]
114. Ogunjuyigbe, A.S.O.; Ayodele, T.R.; Adetokun, B.B.; Jimoh, A.A. Dynamic performance of wind-driven self-excited reluctance generator under varying wind speed and load. In Proceedings of the International Conference on Renewable Energy Research and Applications (ICRERA 2016), Birmingham, UK, 20–23 November 2016; pp. 506–511. [CrossRef]
115. Chirca, M.; Dranca, M.; Breban, S.; Szabó, L. In-wheel Slotless Permanent Magnet Synchronous Motor for Light Electric Vehicle Propulsion. In Proceedings of the International Conference on Modern Power Systems (MPS), Cluj-Napoca, Romania, 21–23 June 2023; pp. 1–4. [CrossRef]
116. Guenoune, I.; Plestan, F.; Chermitti, A.; Evangelista, C. Modeling and robust control of a twin wind turbines structure. *Control Eng. Pr.* **2017**, *69*, 23–35. [CrossRef]
117. Cui, Y.; Song, P.; Wang, X.S.; Yang, W.X.; Liu, H.; Liu, H.M. Wind Power Virtual Synchronous Generator Frequency Regulation Characteristics Field Test and Analysis. In Proceedings of the 2018 2nd International Conference on Green Energy and Applications (ICGEA), Singapore, 24–26 March 2018; pp. 193–196. [CrossRef]
118. Mei, H. The hardware design of the testing system for small grid-off wind turbine generator based on LabVIEW. In Proceedings of the 2011 International Conference on Electronics, Communications and Control (ICECC), Ningbo, China, 9–11 September 2011; pp. 1118–1121. [CrossRef]
119. Fuchs, F.W.; Dannehl, J.; Lohde, R.; Dinkhauser, V.; Jensen, S.; Knop, A.; Wessels, C. Research laboratory for power Electronic generator systems in wind turbines comprising converters, generators, interaction and grid interaction. In Proceedings of the 2009 13th European Conference on Power Electronics and Applications, Barcelona, Spain, 8–10 September 2009; pp. 1–15.
120. Singh, M.; Muljadi, E.; Gevorgian, V. Test cases for wind power plant dynamic models on real-time digital simulator. In Proceedings of the 2012 IEEE Power Electronics and Machines in Wind Applications, Denver, CO, USA, 16–18 July 2012; pp. 1–7. [CrossRef]
121. Yamamoto, Y.; Kobayashi, S.; Yamashita, K.-I. Effects of System Parameters on the Steady-State Characteristics of a Wind Turbine Generator Based on Self-Excited Synchronous Generator for HVDC-Connected Wind Power Plants. In Proceedings of the 2021 24th International Conference on Electrical Machines and Systems (ICEMS), Gyeongju, Republic of Korea, 31 October–3 November 2021; pp. 2223–2227. [CrossRef]

122. Li, H.; Lei, Y.; Geng, Y.; He, H.; Niu, Q.; Wang, K.; Wu, Y. A test methodology to verify reactive power support ability of wind turbines. In Proceedings of the 2022 IEEE 5th International Electrical and Energy Conference (CIEEC), Nangjing, China, 27–29 May 2022; pp. 449–454. [CrossRef]
123. Tammaruckwattana, S.; Ohyama, K. Experimental verification of variable speed wind power generation system using permanent magnet synchronous generator by boost converter circuit. In Proceedings of the IECON 2013—39th Annual Conference of the IEEE Industrial Electronics Society, Vienna, Austria, 10–13 November 2013; pp. 7157–7162. [CrossRef]
124. Cherukuri, H.H.C.; Saravanan, B.; Arunkumar, G. Experimental evaluation of the performance of virtual storage units in hybrid micro grids. *Int. J. Electr. Power Energy Syst.* **2020**, *114*, 105379. [CrossRef]
125. Rastegar, F. Presenting a New Robust Control Structure for Quality Enhancement and Power Mitigation in a Wind Power System. In Proceedings of the 2022 26th International Electrical Power Distribution Conference (EPDC), Tehran, Iran, 11–12 May 2022; pp. 76–83.
126. Allagui, M.; Hasnaoui, O.B.; Belhadj, J. A 2mw direct drive wind turbine; vector control and direct torque control techniques comparison. *J. Energy S. Afr.* **2014**, *25*, 117–126. [CrossRef]
127. Liu, J.; Meng, H.; Hu, Y.; Lin, Z.; Wang, W. A novel MPPT method for enhancing energy conversion efficiency taking power smoothing into account. *Energy Convers. Manag.* **2015**, *101*, 738–748. [CrossRef]
128. Jadidi, S.; Badihi, H.; Zhang, Y. Enhancing Hierarchical Fault-Tolerant Cooperative Control in Wind Farms: The Application of Model Predictive Control and Control Reallocation. In Proceedings of the International Conference on Renewable Energy Research and Applications (ICRERA 2023), Oshawa, ON, Canada, 29 August–1 September 2023; pp. 429–434. [CrossRef]
129. Zamzoum, O.; El Mourabit, Y.; Errouha, M.; Derouich, A.; El Ghzizal, A. Power control of variable speed wind turbine based on doubly fed induction generator using indirect field-oriented control with fuzzy logic controllers for performance optimization. *Energy Sci. Eng.* **2018**, *6*, 408–423. [CrossRef]
130. Bekker, J.C.; Vermeulen, H.J. Parameter estimation of a doubly-fed induction generator in a wind generation topology. In Proceedings of the 47th International Universities Power Engineering Conference (UPEC), Uxbridge, UK, 4–7 September 2012; pp. 1–6. [CrossRef]
131. Wang, X.; Xiong, J.; Geng, L.; Zheng, J.; Zhu, S. Parameter identification of doubly-fed induction generator by the Levenberg-Marquardt-Fletcher method. In Proceedings of the IEEE Power & Energy Society General Meeting, Vancouver, BC, Canada, 21–25 July 2013; pp. 1–5. [CrossRef]
132. Su, J.; Chen, Y.; Sun, L.; Liu, X.; Kang, Y. Parameter estimation of brushless doubly-fed induction generator based on steady experimental results. In Proceedings of the 2015 IEEE Energy Conversion Congress and Exposition (ECCE), Montreal, QC, Canada, 20–24 September 2015; pp. 2800–2804. [CrossRef]
133. Farias, É.R.C.; Cari, E.P.T.; Erlich, I.; Shewarega, F. Online Parameter Estimation of a Transient Induction Generator Model Based on the Hybrid Method. *IEEE Trans. Energy Convers.* **2018**, *33*, 1529–1538. [CrossRef]
134. Su, J.; Du, X.; Fang, L. Integrated parameter estimation method for Brushless doubly-fed induction generator based on simplified d-q model. In Proceedings of the 2021 International Conference on Power System Technology (POWERCON), Haikou, China, 8–9 December 2021; pp. 1388–1393. [CrossRef]
135. *IEEE 115-2019*; IEEE Approved Draft Guide for Test Procedures for Synchronous Machines Including Acceptance and Performance Testing and Parameter Determination for Dynamic Analysis. IEEE: Piscataway, NJ, USA, 2019; pp. 1–232.
136. Agahi, H.; Karrari, M.; Mahmoodzadeh, A. Two New Methods for Synchronous Generator Parameter Estimation. In Proceedings of the IEEE Lausanne Power Tech, Lausanne, Switzerland, 1–5 July 2007; pp. 1061–1066. [CrossRef]
137. Escarela-Perez, R.; Niewierowicz, T.; Campero-Littlewood, E.; Hernandez-Avila, J.L. Estimation of Two-axis Synchronous Machine Parameters using Non-Deterministic Tools. In Proceedings of the 4th International Conference on Electrical and Electronics Engineering, Mexico City, Mexico, 5–7 September 2007; pp. 237–240. [CrossRef]
138. Saied, S.A.; Karrari, M.; Abbaszadeh, K.; Malik, O.P. Identification of electric parameters of synchronous generators with detailed representation of damper windings. In Proceedings of the 40th North American Power Symposium, Calgary, AB, Canada, 28–30 September 2008; pp. 1–6. [CrossRef]
139. Aljabrine, A.; Johnson, B.K.; Fischer, N. Synchronous Generator Testbed for Parameter Estimation. In Proceedings of the 2021 IEEE International Electric Machines & Drives Conference (IEMDC), Hartford, CT, USA, 17–20 May 2021; pp. 1–5. [CrossRef]
140. Das, P.P.; Satpathy, S.; Bhattacharya, S.; Veliadis, V.; Deshpande, U.; Bhargava, B. Determination of Parameters of Symmetrical Six-Phase Permanent Magnet Synchronous Machines. In Proceedings of the IEEE International Electric Machines & Drives Conference (IEMDC), San Francisco, CA, USA, 15–18 May 2023; pp. 1–7. [CrossRef]
141. Zou, Z.; Lu, Q.; Li, Y.; Zhu, Z.Q. Dynamic Regressor Extension and Mixing-Based Parameter Estimation for Permanent Magnet Linear Synchronous Machines Considering Parameter Asymmetry. In Proceedings of the IEEE International Electric Machines & Drives Conference (IEMDC), San Francisco, CA, USA, 15–18 May 2023; pp. 1–6. [CrossRef]
142. Mir, S.; Islam, M.S.; Sebastian, T.; Hussain, I. Self-tuning of machine parameters in switched reluctance motor drives. In Proceedings of the Conference Record of the 2001 IEEE Industry Applications Conference. 36th IAS Annual Meeting (Cat. No.01CH37248), Chicago, IL, USA, 30 September–4 October 2001; Volume 3, pp. 2081–2088. [CrossRef]
143. Viorel, I.-A.; Hameyer, K.; Strete, L. Transverse flux tubular switched reluctance motor. In Proceedings of the 2008 11th International Conference on Optimization of Electrical and Electronic Equipment, Brasov, Romania, 22–24 May 2008; pp. 131–136. [CrossRef]

144. Strete, L.; Husain, I.; Cornea, O.; Viorel, I.-A. Direct and inverse analytical models of a switched reluctance motor. In Proceedings of the Digests of the 2010 14th Biennial IEEE Conference on Electromagnetic Field Computation, Chicago, IL, USA, 9–12 May 2010; p. 1. [CrossRef]
145. Thirumalasetty, M.; Narayanan, G. Experimental Identification of Mechanical Parameters for Speed Controller Design of Switched Reluctance Machine Drive. In Proceedings of the IEEE International Conference on Energy Technologies for Future Grids (ETFG), Wollongong, Australia, 3–6 December 2023; pp. 1–6. [CrossRef]
146. Cebolla, F.J.P.; Martinez, A.; Martin, B.; Laloya, E.; Montano, C.E.; Mendez, S.; Vicuna, J.E. Experimental equivalent circuit parameters identification of a switched reluctance motor. In Proceedings of the 35th Annual Conference of IEEE Industrial Electronics, Porto, Portugal, 3–5 November 2009; pp. 1140–1145. [CrossRef]
147. Ding, Y.; Yu, K.; Tao, N.; Wang, J.; Palanas, P.J.; Xie, X. Operation Control Strategies for Switched Reluctance Motor Driven Flywheel Energy Storage System with Switching Angle Optimization. In Proceedings of the 4th International Conference on Electrical Engineering and Control Technologies (CEECT), Shanghai, China, 17 December 2022; pp. 1013–1019. [CrossRef]